Title

MicroRNA regulation of type 2 innate lymphoid cell homeostasis and function in allergic inflammation

Journal

Journal of Experimental Medicine, 214(12)

ISSN

0022-1007

Authors

Singh, Priti B

Pua, Heather H

Happ, Hannah C

et al.

Publication Date

2017-12-04

DOI

10.1084/jem.20170545

Peer reviewed

MicroRNA regulation of type 2 innate lymphoid cell homeostasis and function in allergic inflammation

Priti B. Singh,[1,5] Heather H. Pua,[2,5] Hannah C. Happ,[1,5] Christoph Schneider,[3] Jakob von Moltke,[3] Richard M. Locksley,[3,4,5] Dirk Baumjohann,[6] and K. Mark Ansel[1,5]

[1]Department of Microbiology and Immunology, [2]Department of Pathology, [3]Department of Medicine, [4]Howard Hughes Medical Institute, and [5]Sandler Asthma Basic Research Center, University of California, San Francisco, San Francisco, CA
[6]Institute for Immunology, Biomedical Center Munich, Ludwig-Maximilians-Universität München, Planegg-Martinsried, Germany

MicroRNAs (miRNAs) exert powerful effects on immunity through coordinate regulation of multiple target genes in a wide variety of cells. Type 2 innate lymphoid cells (ILC2s) are tissue sentinel mediators of allergic inflammation. We established the physiological requirements for miRNAs in ILC2 homeostasis and immune function and compared the global miRNA repertoire of resting and activated ILC2s and T helper type 2 (T_H2) cells. After exposure to the natural allergen papain, mice selectively lacking the miR-17∼92 cluster in ILC2s displayed reduced lung inflammation. Moreover, miR-17∼92–deficient ILC2s exhibited defective growth and cytokine expression in response to IL-33 and thymic stromal lymphopoietin in vitro. The miR-17∼92 cluster member miR-19a promoted IL-13 and IL-5 production and inhibited expression of several targets, including SOCS1 and A20, signaling inhibitors that limit IL-13 and IL-5 production. These findings establish miRNAs as important regulators of ILC2 biology, reveal overlapping but nonidentical miRNA-regulated gene expression networks in ILC2s and T_H2 cells, and reinforce the therapeutic potential of targeting miR-19 to alleviate pathogenic allergic responses.

The Journal of Experimental Medicine

INTRODUCTION

Type 2 innate lymphoid cells (ILC2s) are a potent source of the type 2 signature cytokines IL-13 and IL-5 that drive allergic inflammation (Scanlon and McKenzie, 2012; Diefenbach et al., 2014; Klose and Artis, 2016). ILC2s are present in sputum and bronchoalveolar lavage (BAL) in human asthma (Christianson et al., 2015; Gordon et al., 2016; Smith et al., 2016). They respond to the epithelial cell–derived cytokines IL-33, IL-25, and thymic stromal lymphopoietin (TSLP) and may play a role in the initiation and/or maintenance of chronic airway inflammation. The mechanisms underlying ILC2 development, homeostasis, and function have been the subject of intense investigation. The signaling modules and transcriptional programs that control ILC2 biology bear striking resemblance to those operative in tissue-homing T_H2 cells that mediate similar functions in adaptive immunity (Van Dyken et al., 2016). However, very little is known about the posttranscriptional regulation of ILC2 gene expression and immune function.

MicroRNAs (miRNAs) are ubiquitous posttranscriptional repressors of gene expression that play critical roles in lymphocyte homeostasis and allergic responses (Deshpande et al., 2015; Pua and Ansel, 2015). Each miRNA regulates multiple mRNA targets, and individual mRNAs may be regulated by multiple miRNAs. In this way, miRNA-directed regulatory networks powerfully influence biological processes despite the modest quantitative effect produced by each miRNA-target interaction. ILC2s express miR-155, and miR-155–deficient mice exhibit defective ILC2 and T_H2 cell expansion and allergic airway (AA) inflammation (Okoye et al., 2014; Johansson et al., 2017). However, the expression and function of miRNAs in ILC2s remains largely unexplored.

The miR-17∼92 cluster of miRNAs is a particularly potent and pleiotropic regulator of B and T cell development, proliferation, survival, activation, differentiation, and cytokine production (Mogilyansky and Rigoutsos, 2013). The cluster is transcribed as a single primary miRNA transcript that is processed by the Drosha/Dgcr8 microprocessor complex and Dicer to produce six distinct mature miRNAs. These miRNAs can be classified by their target-determining seed sequences into four families: the miR-17 family (miR-17 and miR-20a), the miR-18 family (miR-18a), the miR-19 family (miR-19a and miR-19b-1), and the miR-92 family (miR-92a-1). miR-19a is uniquely up-regulated in airway-infiltrating T cells from asthmatic subjects, and it promotes T_H2 cell cytokine production at least in part through direct targeting of the signaling inhibitors *Pten*, *Socs1*, and *Tnfaip3* (which encodes A20; Simpson et al., 2014).

In the current study, we profiled and compared the miRNA transcriptomes of lung ILC2s and T_H2 cells. miRNA expression was absolutely required to maintain ILC2 homeostasis in vivo, and the miR-17∼92 cluster was partially

Correspondence to K. Mark Ansel: mark.ansel@ucsf.edu

Abbreviations used: AA, allergic airway; BAL, bronchoalveolar lavage; ILC2, type 2 innate lymphoid cell; miRNA, microRNA; rpm, reads per million; TSLP, thymic stromal lymphopoietin.

The Rockefeller University Press
J. Exp. Med. 2017 Vol. 214 No. 12 3627–3643
https://doi.org/10.1084/jem.20170545

responsible for this function. In addition, miR-17∼92 promoted IL-13 and IL-5 production in response to IL-33 and ILC2-driven type 2 inflammation in vivo. We established RNA transfection of ILC2s and showed that miR-19a or siRNAs against its targets, *Socs1* or *Tnfaip3*, can rescue the defective cytokine production of miR-17∼92–deficient ILC2s. We conclude that miRNAs are crucial regulators of ILC2 biology that mediate similar but nonidentical programs of posttranscriptional gene regulation in innate and adaptive lymphocytes.

RESULTS

ILC2 miRNAome shares features with T_H2 cells

Small RNA sequencing was performed to define the ILC2 miRNAome. RNA was obtained from $CD45^+Lin^-$ $Thy1.2^+CD4^-ST2^+CD25^+$ ILC2s sorted from dissociated mouse lung tissue with or without three consecutive days of oropharyngeal IL-33 treatment. IL-33 instillation in the lungs expands and activates ILC2s (Bartemes et al., 2012; Kamijo et al., 2013), and we consistently recovered approximately twice as many ILC2s after IL-33 treatment. ILC2s were also analyzed after in vitro culture for 10 d in IL-33, TSLP, and IL-7. For comparison, RNA was collected from $CD4^+CD25^-$ $CD62L^{hi}CD44^{lo}$ naive T cells from spleen and lymph nodes; $CD4^+4get^+$ T_H2 cells from BAL after the induction of AA inflammation in 4get mice containing a bicistronic mRNA linking a readily identifiable reporter, enhanced GFP (EGFP), to IL-4 gene expression (Mohrs et al., 2001); and in vitro differentiated T_H2 cells. Among all samples, 46–95% of sequence reads that mapped to the genome aligned to mature miRNAs. Contaminating rRNA, tRNA, and mRNA fragments comprised, on average, just 9%, 4%, and 5% of mapped reads, respectively (Table S1).

Overall, there was a strong positive correlation between the global miRNA expression profiles of all ILC2 and T cell samples (Fig. 1 A). However, pairwise comparisons revealed differences between sample groups (Table S2). Unsupervised hierarchical clustering of 147 miRNAs with significant differential expression (adjusted $P < 0.01$) in any pair of sample groups clustered the data by cell type (Fig. 1 B). Blocks of miRNAs with a shared signature were highlighted by this analysis, the largest being an "ILC2" block, a naive "CD4" block, and an "in vitro" block common to cultured ILC2 and T cells (Table S3). The expression profiles of ILC2s and ILC2s harvested after IL-33 administration in vivo were nearly identical. However, 14 miRNAs were significantly differentially expressed in ILC2s after 10 d of in vitro culture in IL-33 (Fig. 1 C and Table S2).

The expression of this group of 14 miRNAs was also investigated in naive $CD4^+$ T cells and in vitro–cultured T_H2 cells, revealing both shared and unique expression changes after in vitro activation of ILC2s and their adaptive lymphoid counterparts. miR-21a, miR-98, and miR-155 were similarly up-regulated, and miR-203, miR-151, and let-7c were similarly down-regulated, in both ILC2s and T_H2 cells (Fig. 1 C). miR-150 was also down-regulated in both cell types, though the effect size was larger in T_H2 cells. Quantitative PCR analyses confirmed that miR-150 was down-regulated, and miR-155 and miR-21 up-regulated, in ILC2s cultured for 10 d in IL-33 (Fig. 1 D). miR-146, a feedback inhibitor of NF-κB signaling that can be up-regulated in activated T cells under some conditions (Curtale et al., 2010; Rusca et al., 2012; Yang et al., 2012), was also up-regulated in ILC2s cultured in IL-33, but not in T cells cultured in T_H2-polarizing conditions (Fig. 1 C; Monticelli et al., 2005).

A few miRNAs exhibited markedly different expression and regulation patterns in ILC2s and T cells. miR-126a expression was down-regulated from a mean of 8,000 reads per million (rpm) to 200 rpm after ILC2 culture in IL-33, but was up-regulated from 10 rpm in naive $CD4^+$ T cells to 100 rpm during in vitro T_H2 cell differentiation (Fig. 1 C and Table S4). In addition, three members of the large *Mirc7* miRNA cluster on mouse chromosome 12, miR-541, miR-409, and miR-134, had very low baseline expression in ILC2s and naive $CD4^+$ T cells but were up-regulated more than 100-fold in cultured ILC2s. These miRNAs remained poorly expressed in cultured T_H2 cells, but they were expressed in $4get^+$ T_H2 cells freshly isolated from AA samples at ∼30-fold higher abundance than in naive $CD4^+$ T cells. The remaining members of the *Mirc7* cluster were all expressed in relatively low amounts, typically <10 rpm. Full aligned miRNA sequence data are compiled in Table S4.

Severe reduction of lung ILC2s in miRNA-deficient mice

To investigate the overall requirements for miRNAs in ILC2 biology, we generated mice that lack the essential canonical miRNA biogenesis factor Dgcr8 in fluorescently marked ILC2s (hereafter termed $Dgcr8^{\Delta/\Delta}$). Conditional *Dgcr8*-deficient mice (Rao et al., 2009) were intercrossed with Red5 mice (Nussbaum et al., 2013) in which *Il5* is replaced with sequences encoding Cre recombinase and the fluorescent protein tdTomato, and with R26-YFP transgenic mice (Luche et al., 2007) to introduce a durable reporter of Cre expression. Total ILC2s in the lungs of $Dgcr8^{+/-}$ (*Dgcr8*-sufficient controls) and $Dgcr8^{\Delta/\Delta}$ (*Dgcr8*-deficient) mice were analyzed as live $CD45^+$ $CD90^+lin^-CD4^-CD25^+$ (Fig. 2 A). Lung ILC2s identified in this way also expressed the IL-33 receptor, ST2 (Fig. 2 B). Global loss of canonical miRNAs in these cells severely impaired ILC2 homeostasis. Flow cytometric analyses showed a marked reduction of total lung ILC2s in $Dgcr8^{\Delta/\Delta}$ mice compared with *Dgcr8*-sufficient controls (Fig. 2 C). A very severe defect was revealed by restricting analysis to YFP^+ ILC2s, indicating that *Dgcr8* deficiency is incompatible with long-term ILC2 survival (Fig. 2 D). Further analysis of the impact of miRNA deficiency on ILC2 function in these animals was precluded by the near absence of YFP^+ $Dgcr8^{\Delta/\Delta}$ ILC2s (Fig. 2 E). Even ILC2s that expressed the *Red5* tdTomato but had not yet established R26-YFP reporter expression were affected (Fig. 2 F). In contrast, there was no difference in the frequency of YFP^-Red5^- ILC2s that

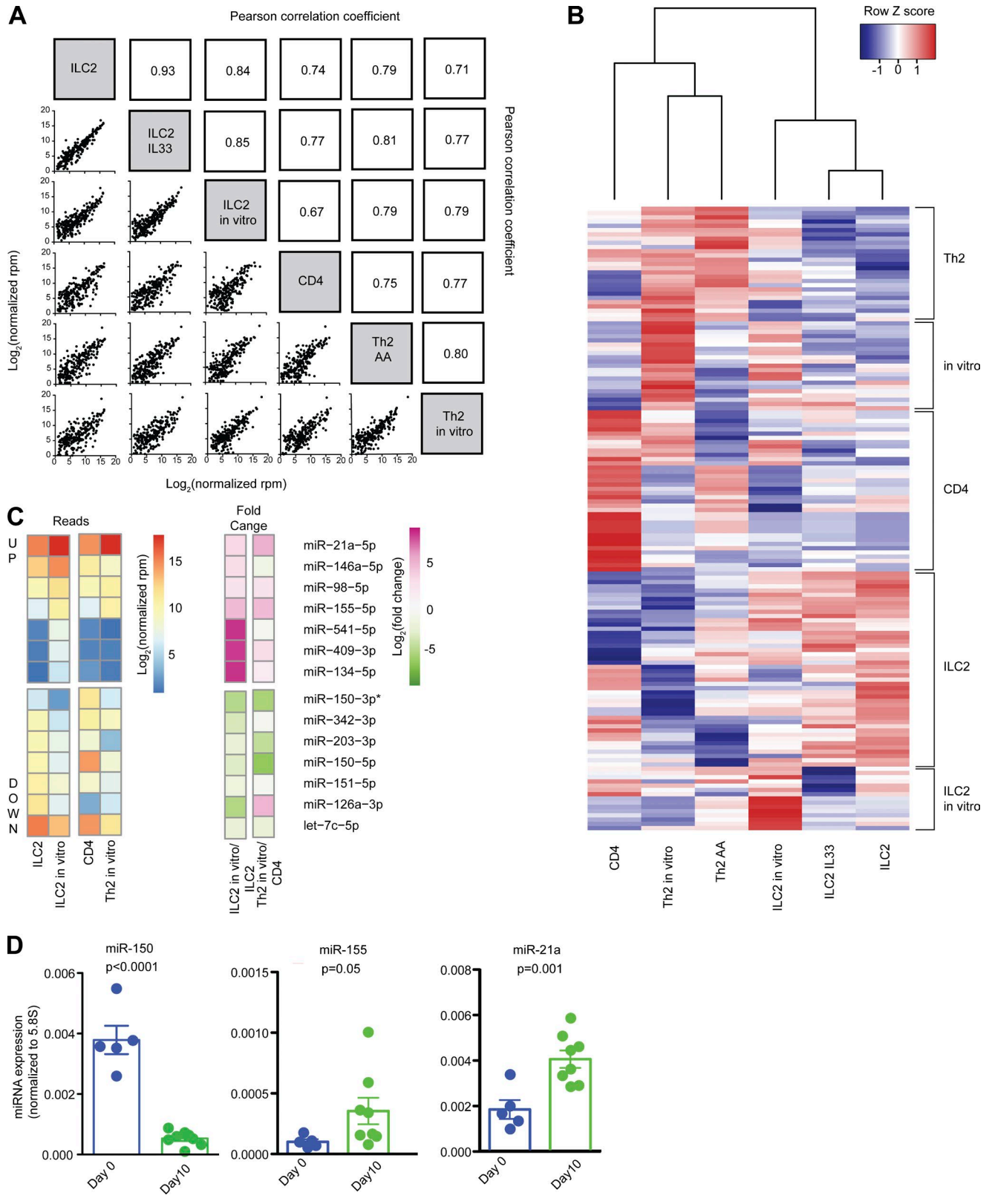

Figure 1. **Small RNA sequencing expression analysis of miRNAs in ILC2s and T cells.** (A) Pearson correlation coefficients for global miRNA expression profiles among all samples. Sample groups include ILC2s isolated from naive mouse lung (ILC2), ILC2s isolated from mouse lung after IL-33 treatment (ILC2 IL33), ILC2 cultured in vitro for 10 d (ILC2 in vitro), naive CD4 T cells (CD4), T_H2 cells isolated from BAL of mice with AAs (T_H2 AA), and T_H2 cells polarized

lack evidence of current or prior Cre expression, indicating that ILC2s that retain miRNA expression did not expand to fill the niche left vacant by *Dgcr8*-deficient ILC2s. Collectively, these results demonstrate that *Dgcr8* deletion leads to ILC2 depletion, underscoring the importance of miRNA biogenesis for the maintenance of normal ILC2s in the lung.

The miR-17∼92 cluster regulates lung ILC2 homeostasis

Because of the severity of the defect caused by *Dgcr8* deficiency, further investigation of miRNA regulation of ILC2 immune function requires examination of specific miRNAs expressed in ILC2s. The miR-17∼92 cluster of miRNAs exert powerful effects on lymphocyte homeostasis, differentiation, and effector function, including T_H2 cell cytokine production (Mogilyansky and Rigoutsos, 2013; Simpson et al., 2014). All six mature miRNA members of the miR-17∼92 cluster (miR-17, miR-18a, miR-19a, miR-20a, miR-19b-1, and miR-92a-1; Fig. 3 A) were expressed in freshly isolated and IL-33–stimulated ILC2s at abundances similar to those expressed in naive $CD4^+$ T cells and T_H2 cells (Fig. 3 B). To determine whether the miR-17∼92 cluster regulates ILC2 homeostasis and function, we intercrossed mice in which the entire miR-17∼92 cluster is flanked by loxP sites with Red5 mice (hereafter termed $17{\sim}92^{\Delta/\Delta}$). In addition, Cre-activatable R26–miR-17∼92 transgenic mice were intercrossed with Red5 mice to generate animals with fluorescently marked $17{\sim}92^{tg/tg}$ ILC2s overexpressing the miR-17∼92 cluster. miR-17∼92 cluster miRNA expression in $Red5^+$ $17{\sim}92^{\Delta/\Delta}$ ILC2s was below the limit of detection or very low compared with miR-17∼92–sufficient control $Red5^+$ $17{\sim}92^{+/+}$ ILC2s (Fig. 3 C).

The miR-17∼92 cluster regulated the maintenance of lung ILC2s. The frequency of total and $Red5^+$ ILC2s was reduced by almost 50% in $17{\sim}92^{\Delta/\Delta}$ mouse lungs compared with miR-17∼92–sufficient $Red5^+$ $17{\sim}92^{+/+}$ control mice (Fig. 3 D). Conversely, $17{\sim}92^{tg/tg}$ mice bore more than twice the normal number of total and $Red5^+$ ILC2s (Fig. 3 E). Thus, miR-17∼92 cluster miRNAs account for a significant proportion of the miRNA requirements for lung ILC2 homeostasis, although other miRNAs must also play major roles in this process.

The miR-17∼92 cluster promotes ILC2 function in AA inflammation

Tissue-resident ILC2 cells expand and secrete IL-5 and IL-13 in response to agents that incite type 2 inflammation. We used a mouse model of AA inflammation to test the generation and function of ILC2s in vivo and investigate the requirements for miR-17∼92 in an ILC2-mediated type 2 response. Mouse airways were challenged with the allergen papain on three consecutive days, and lung tissue samples were harvested on day 4 (Fig. 4 A). ILC2s expanded in response to papain in both $17{\sim}92^{+/+}$ and $17{\sim}92^{\Delta/\Delta}$ mice, although the total number of ILC2s present in the lung was significantly lower in $17{\sim}92^{\Delta/\Delta}$ mice (Fig. 4 B). To characterize and quantify airway inflammation, we analyzed BAL and digested lung tissue cells by flow cytometry. Airway and lung eosinophil infiltration was reduced in $17{\sim}92^{\Delta/\Delta}$ mice, whereas $CD4^+$ T cell numbers were similar in both groups of mice (Fig. 4, C and D). Consistent with the observed type 2 inflammation, IL-13 was significantly induced by papain in the BAL fluid of $17{\sim}92^{+/+}$, but not $17{\sim}92^{\Delta/\Delta}$ mice (Fig. 4 E). IL-5 protein was induced in the BAL of both groups of mice, but the *Il5* mRNA was more abundant in $17{\sim}92^{+/+}$ total lung cells (Fig. 4 F). *Il13* mRNA exhibited a similar trend but did not reach statistical significance. Papain-treated $17{\sim}92^{\Delta/\Delta}$ mice exhibited significantly reduced frequencies of $IL\text{-}5^+$, $IL\text{-}13^+$, and IL-5/IL-13 double-positive lung ILCs compared with $17{\sim}92^{+/+}$ control mice (Fig. 4 G). Thus, miR-17∼92 deficiency in ILC2s decreased type 2 cytokine expression and eosinophilia, the hallmarks of allergic lung inflammation.

To observe lung pathology, mice were challenged with papain on days 1, 3, and 5, and lung samples were harvested for histology 6 d after the initiation of papain treatment (Fig. 4 H). A persistent reduction in total inflammation was observed in $17{\sim}92^{\Delta/\Delta}$ mice (Fig. 4 I). Only sparse focal epithelial cell mucus metaplasia was observed by periodic acid–Schiff staining in tissue sections of either $17{\sim}92^{+/+}$ or $17{\sim}92^{\Delta/\Delta}$ mice, precluding quantitative analysis (not depicted). However, IL-13–responsive genes that promote mucus production and tissue repair, including *Muc5ac*, *Clca3*, and *Gob5* (Kuperman et al., 2002; Thai et al., 2005), were significantly lower in the epithelial brushings of papain-challenged $17{\sim}92^{\Delta/\Delta}$ mice (Fig. 4 J). Collectively, these data show that the miR-17∼92 cluster promotes the in vivo function of ILC2s in the induction of AA inflammation. Because a minor fraction of ILC2s remained $Red5^-$ in papain-challenged mice (Fig. 4 B), these results may underestimate the physiological effect of miR-17∼92 deficiency in ILC2s.

The miR-17∼92 cluster promotes ILC2 growth and regulates cytokine production

To understand the mechanisms by which the miR-17∼92 cluster promotes ILC2-mediated type 2 immune responses, equal numbers of lung ILC2s from $17{\sim}92^{+/+}$ or $17{\sim}92^{\Delta/\Delta}$ mice were purified and cultured in IL-33, TSLP, and IL-7.

in vitro (T_H2 in vitro). (B) Unsupervised hierarchical clustering of all DESeq2 differentially expressed miRNAs. A list of individual miRNAs in each subgroup is included in Table S2. (C) Heat map of $\log_2$ normalized read counts and fold changes of miRNAs significantly (adjusted $P < 0.01$) up- or down-regulated in ILC2s after culture in vitro with IL-33, TSLP, and IL-7. Values for naive CD4 T cells and T cells after 5 d of T_H2 polarizing culture are also provided for comparison. (D) Quantitative PCR confirmation of RNA sequencing data for the indicated miRNAs. Bars represent mean ± SEM. P-values were calculated with Student's *t* test.

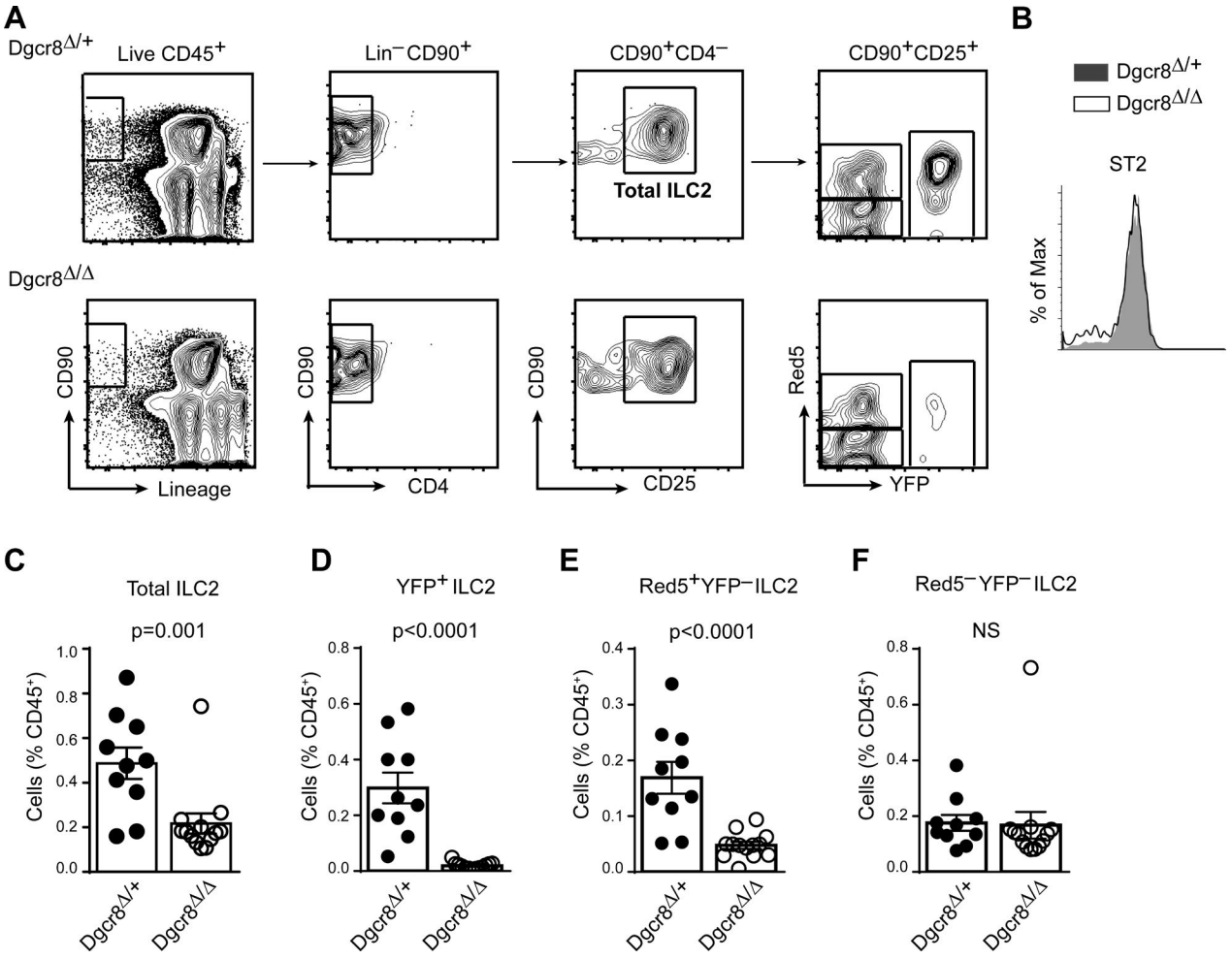

Figure 2. **Severe reduction of lung ILC2s in Red5 *Dgcr8*$^{\Delta/\Delta}$ mice.** (A) Contour plots depict the gating strategy for lung ILC2s in *Dgcr8*$^{\Delta/+}$ and *Dgcr8*$^{\Delta/\Delta}$ mice. Total ILC2s are identified as live CD45$^+$CD90$^+$lin$^-$CD4$^-$CD25$^+$ cells. Among total ILC2s, tdTomato (Red5) fluorescence indicates Cre expression, and YFP expressed from the R26-YFP reporter indicates Cre activity. (B) Flow cytometric analysis of ST2 median fluorescence intensity (MFI) in the total ILC2s of *Dgcr8*$^{\Delta/+}$ and *Dgcr8*$^{\Delta/\Delta}$ lung. (C–F) Flow cytometric quantification of total ILC2s (C), YFP$^+$ ILC2s (D), Red5$^+$ YFP$^-$ILC2s (E), and Red5$^-$ YFP$^-$ILC2s (F) in the lung of *Dgcr8*$^{\Delta/+}$ and *Dgcr8*$^{\Delta/\Delta}$ mice. Bar graphs show ILC2 frequency as percentage of live CD45$^+$ cells (mean ± SEM). Each data point represents an individual mouse. Data were pooled from two independent experiments each with five to seven mice per group. P-values were calculated with Student's *t* test.

17∼92$^{\Delta/\Delta}$ ILC2s expressed ST2, TSLPR, and IL7R normally (not depicted). These stimuli induced ILC2 proliferation in vitro, but fewer fluorescent Red5$^+$ cells were visible in 17∼92$^{\Delta/\Delta}$ cultures within 4 d (Fig. 5 A). We used CyQUANT assays to accurately measure ILC2s outgrowth in vitro, revealing a 60% reduction in the 17∼92$^{\Delta/\Delta}$ ILC2s present at day 4 compared with control 17∼92$^{+/+}$ cultures (Fig. 5 B). Similar results were observed throughout the 10-d culture period. To test whether the miR-17∼92 cluster affected ILC2 proliferation, we examined Ki67 expression at day 3. A significantly higher percentage of 17∼92$^{+/+}$ ILC2s were Ki67$^+$ compared with 17∼92$^{\Delta/\Delta}$ ILC2s (Fig. 5 C). Annexin V staining indicated no difference in the rate of apoptosis (Fig. 5, D and E). These data indicate that miR-17∼92 is required for normal cytokine-driven ILC2 proliferation in vitro.

ILC2 cytokine production was also independently affected by miR-17∼92 deficiency. 17∼92$^{\Delta/\Delta}$ ILC2s produced less IL-13, IL-6, and GM-CSF over 10 d of culture (Fig. 6 A). Because there were fewer ILC2s present in 17∼92$^{\Delta/\Delta}$ cultures at day 4, we also measured early cytokine secretion at day 2 and observed a similar result (Fig. 6 B). Conversely, 17∼92$^{tg/tg}$ ILC2s produced more IL-13, IL-6, and GM-CSF than did their 17∼92$^{+/+}$ counterparts at 10 d of culture (Fig. 6 C). IL-2, IL-4, and IL-10 were not detected in these culture conditions. For further confirmation and to determine whether cytokine expression differences could be observed on a per-cell basis independent of cell number, we also measured cytokine transcripts. Indeed, 17∼92$^{\Delta/\Delta}$ ILC2s exhibited reduced *Il13* mRNA expression (Fig. 6 D), and 17∼92$^{tg/tg}$ ILC2s had increased *Il13* expression compared with control 17∼92$^{+/+}$

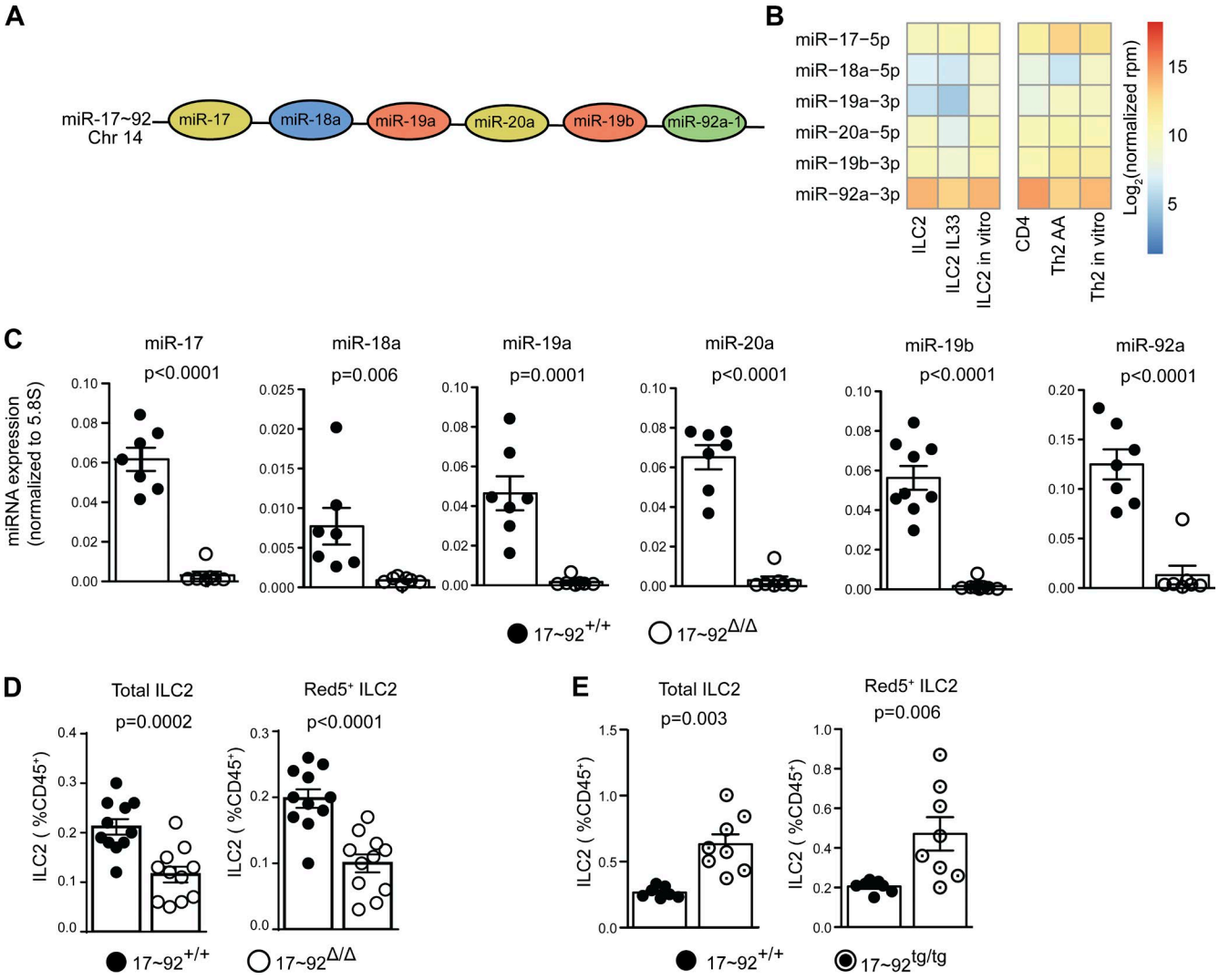

Figure 3. **miR-17~92 cluster expression and requirement in lung ILC2s.** (A) Schematic of the miR-17~92 cluster miRNAs and their chromosomal positions. Colors indicate miRNAs families. (B) Heat map of log2 normalized read counts of miR-17~92 cluster miRNAs in the indicated cell types (see Fig. 1 legend). (C) Quantitative PCR quantification of the indicated miRNAs in 10-d-cultured 17~92$^{\Delta/\Delta}$ and 17~92$^{+/+}$ ILC2s. Symbols indicate individual cultures seeded with cells from a pool of two to three mice each. Data were pooled from three independent experiments. (D and E) Flow cytometric quantification of total lung ILC2 and Red5^{+} ILC2 frequency (see Fig. 2 A legend) in 17~92$^{\Delta/\Delta}$ (D) and 17~92$^{tg/tg}$ (E) mice compared with matched 17~92$^{+/+}$ controls. Each ILC2 culture was started with 10,000 (B) or 3,500 (C) ILC2s sorted from individual mouse or pools of two to six mice and cultured with IL-33, TSLP, and IL-7 for 10 d. Each data point represents the ILC2 frequency expressed as percentage of live CD45^{+} cells in an individual mouse. Data were pooled from two independent experiments. Bars represent mean ± SEM. P-values were calculated with Student's *t* test.

ILC2s (Fig. 6 E). However, this defect was specific to *Il13*, as 17~92$^{\Delta/\Delta}$ ILC2s expressed higher levels of *Il6, Csf2* (which encodes GM-CSF), and *Il9* (Fig. 6 D). Consistent with these data, 17~92$^{tg/tg}$ ILC2s had decreased expression of *Csf2* and *Il9* compared with control 17~92$^{+/+}$ ILC2s (Fig. 6 E). The enhanced expression of *Il6, Csf2*, and *Il9* in 17~92$^{\Delta/\Delta}$ ILC2s indicates that they were fully capable of cytokine expression in response to IL-33, TSLP, and IL-7 in vitro, yet they display a specific defect in the production of type 2 cytokines. 17~92$^{\Delta/\Delta}$ ILC2s also showed a per-cell reduction in IL-5 expression as indicated by reduced *Red5*-encoded tdTomato fluorescence intensity (Fig. 6 F). Consistent with previous findings in T_H2 cells, miR-17~92 did not affect GATA-3 expression in ILC2s (Fig. 6 G). Collectively, these data demonstrate important roles for the miR-17~92 cluster in promoting ILC2 proliferative capacity and regulating cytokine production.

miR-19a promotes IL-13 and IL-5 production in ILC2s

The miR-17~92 cluster promotes type 2 cytokine expression in T_H2 cells, mainly as a result of the function of the miR-19 family (Simpson et al., 2014). We established a protocol for next-generation transfection of ILC2s with

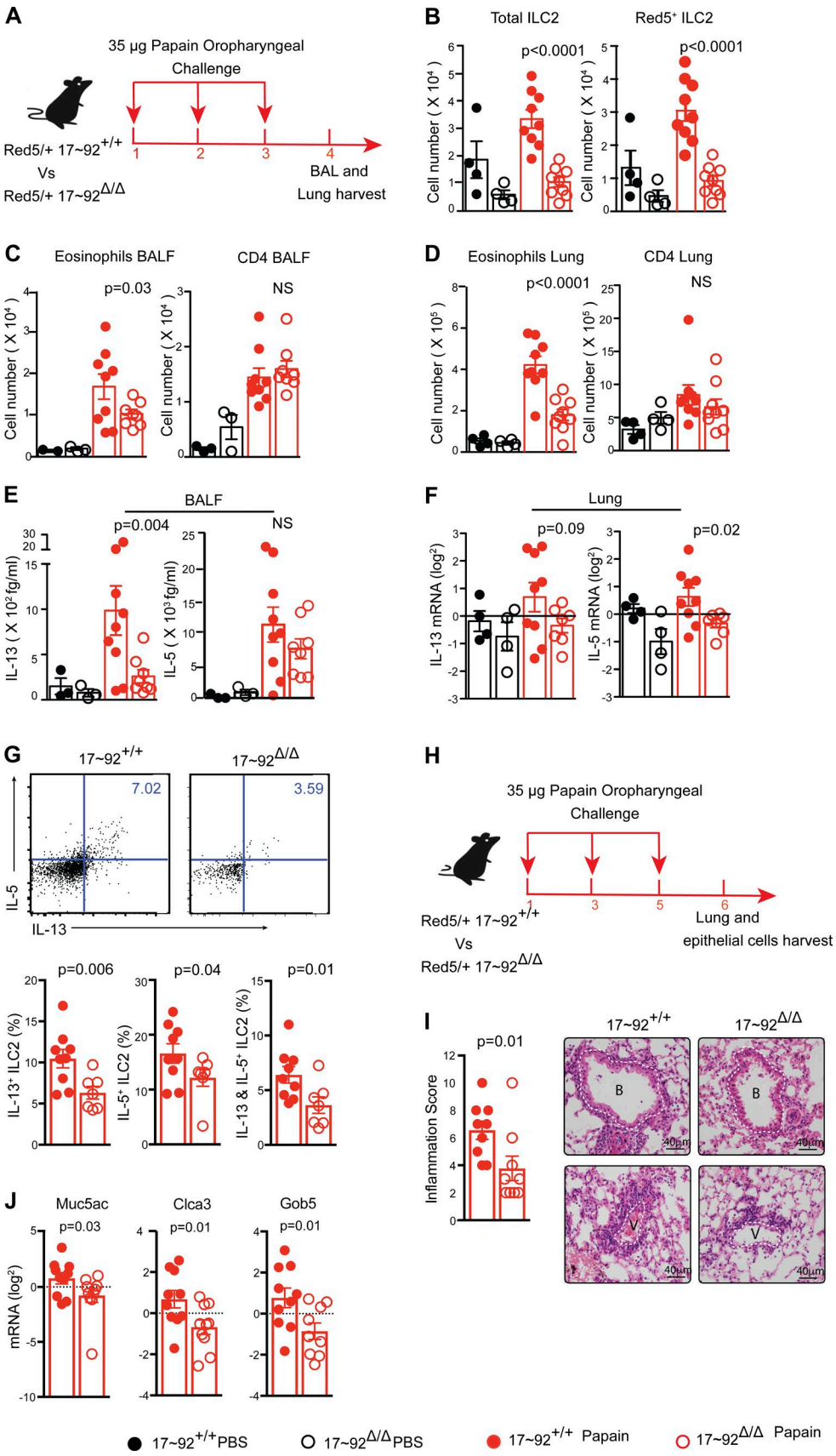
A
35 µg Papain Oropharyngeal Challenge
Red5/+ 17~92+/+
Vs
Red5/+ 17~92Δ/Δ
1
2
3
4
BAL and Lung harvest
B
Total ILC2
Red5+ ILC2
p<0.0001
p<0.0001
Cell number (X 10⁴)
C
Eosinophils BALF
CD4 BALF
p=0.03
NS
Cell number (X 10⁴)
D
Eosinophils Lung
CD4 Lung
p<0.0001
NS
Cell number (X 10⁵)
E
BALF
p=0.004
NS
IL-13 (X 10² fg/ml)
IL-5 (X 10³ fg/ml)
F
Lung
p=0.09
p=0.02
IL-13 mRNA (log²)
IL-5 mRNA (log²)
G
17~92+/+
17~92Δ/Δ
7.02
3.59
IL-5
IL-13
p=0.006
p=0.04
p=0.01
IL-13+ ILC2 (%)
IL-5+ ILC2 (%)
IL-13 & IL-5+ ILC2 (%)
H
35 µg Papain Oropharyngeal Challenge
Red5/+ 17~92+/+
Vs
Red5/+ 17~92Δ/Δ
1
3
5
6
Lung and epithelial cells harvest
I
p=0.01
Inflammation Score
17~92+/+
17~92Δ/Δ
B
V
40µm
J
Muc5ac
Clca3
Gob5
p=0.03
p=0.01
p=0.01
mRNA (log²)
17~92+/+PBS
17~92Δ/ΔPBS
17~92+/+ Papain
17~92Δ/Δ Papain

small RNAs and used it to restore miR-17~92 family members' activity in 17~92$^{\Delta/\Delta}$ ILC2s by transfecting them with miR-19a, miR-18a, miR-17, and miR-92a mimics (Fig. 7 A). All four miRNA mimics increased *Il13* mRNA expression in 17~92$^{\Delta/\Delta}$ ILC2s compared with control mimics, although miR-19a transfection induced *Il13* expression the most (Fig. 7 B). miR-19a transfection also significantly increased *Il5* mRNA expression (Fig. 7 C), but it did not affect *Il6* (Fig. 7 D). 17~92$^{\Delta/\Delta}$ ILC2s transfected with miR-19a mimic secreted significantly more IL-13 (Fig. 7 E) and IL-5 (Fig. 7 F), but not IL-6 protein (Fig. 7 G), than cells transfected with control mimic. Importantly, miR-19a rescued defective IL-13 and IL-5 production in the absence of other endogenous miR-17~92 family miRNAs, even though it was delivered after 8 d of culture. 17~92$^{\Delta/\Delta}$ ILC2s transfected with miR-19a also exhibited significantly higher expression of Ki67 mRNA than control cells transfected with control mimic, indicating that miR-19a affects ILC2 proliferation as well (Fig. 7 H). We conclude that miR-19a is an important member of the miR-17~92 cluster that promotes proliferation and enhances IL-13 and IL-5 production by ILC2s in a cell-intrinsic manner.

miR-19a targets genes that limit IL-13 and IL-5 production in ILC2s

To investigate how miR-19 regulates IL-13 production in ILC2s, a candidate gene approach was taken. We tested several miR-19 target genes that had been previously confirmed in other cell types (Hsu et al., 2011). The mRNAs encoding four of these candidates (*Tnfaip3*, *Socs1*, *Rora*, and *Kit)* were more abundant in cultured 17~92$^{\Delta/\Delta}$ ILC2s than in control 17~92$^{+/+}$ ILC2s (Fig. 8 A), consistent with targeting by one or more miR-17~92 cluster miRNAs in ILC2s. miR-19 was sufficient to mediate repression of *Tnfaip3*, *Socs1*, *Rora*, and *Kit* in 17~92$^{\Delta/\Delta}$ ILC2s, as transfection with miR-19a mimic significantly reduced the expression of their corresponding mRNAs compared with cells transfected with control mimic (Fig. 8 B). Surprisingly, the well-known miR-19 target *Pten* was affected by neither miR-17~92 deficiency nor miR-19a mimic transfection in ILC2s (Fig. 8, A and B).

The functional impact of miR-19 targets on ILC2 cytokine expression was tested by transfecting 17~92$^{\Delta/\Delta}$ ILC2s with siRNAs against *Tnfaip3* and *Socs1*. Compared with control siRNA, *Tnfaip3* and *Socs1* siRNAs increased both IL-13 and IL-5 cytokine production and mRNA expression in ILC2s (Fig. 9, A and B). Thus, these two miR-19 targets specifically regulated IL-13 and IL-5 production in ILC2s. Collectively, these data indicate that miR-19 promotes type 2 cytokine production and regulates overlapping but nonidentical sets of functionally relevant target genes in ILC2 and T_H2 cells.

DISCUSSION

Extensive study of ILC2s in recent years has changed our perception of T_H2 cells as the central cytokine-secreting drivers of allergic inflammation. ILC2s have emerged as a potent early source of type 2 cytokines, important contributors to airway disease models, and a potential link between innate and adaptive phases of type 2 responses (Scanlon and McKenzie, 2012; Martinez-Gonzalez et al., 2015). Several key transcription factors and cytokine signals required for ILC2 development and maturation have been identified, yet knowledge of the gene expression networks that govern ILC2 biology remains underdeveloped (Walker and McKenzie, 2013; von Moltke and Locksley, 2014). In the current study, we demonstrate that miRNAs are absolutely critical regulators of ILC2 homeostasis, and the miRNAs of the miR-17~92 cluster in particular are required for normal ILC2 survival, cytokine production, and allergic responses. One of these, miR-19, promoted IL-13 production and targeted inhibitors of the NF-κB and STAT pathways that mediate innate cytokine signals upstream of *Il13* expression in ILC2s. These findings illustrate how the network logic of miRNA function allows them to regulate common biological outcomes through overlapping but distinct target gene repertoires in different cellular contexts, such as ILC2s and T_H2 cells.

The expression and importance of miRNAs in T, B, and natural killer cells has been well established (Fehniger et al., 2010; Baumjohann and Ansel, 2013; Beaulieu et al., 2013; de Yébenes et al., 2013) but miRNAs were heretofore largely unexplored in other lymphocytes. Global disruption

Figure 4. **miR-17~92 cluster enhances ILC2 function in AA inflammation.** (A) 4-d experimental model of papain-induced airway inflammation. Red5 heterozygous 17~92$^{\Delta/\Delta}$ and 17~92$^{+/+}$ mice received 35 µg papain in 40 µl PBS or PBS alone oropharyngeally on three consecutive days, and lung tissue samples were harvested on day 4. (B) Flow cytometric enumeration of total ILC2s and Red5$^+$ ILC2s in the lung. (C and D) Flow cytometric quantification of the number of eosinophils (Siglec-F$^+$CD11c$^-$) and CD4$^+$ T cells recovered in BAL (C) and digested lung tissue (D). (E) Cytometric bead array (CBA) measurement of IL-13 and IL-5 in BAL fluid. (F) Quantitative PCR (qPCR) quantification of *Il13* and *Il5* mRNA in total lung cells, normalized to *Gapdh* mRNA. (G) Representative flow cytometric analysis of intracellular cytokine staining (top). Numbers in quadrants indicate percentage of cytokine-producing live, Lin$^-$CD45$^+$CD90$^+$CD4$^-$ ILCs. Bar graphs (bottom) show frequencies of lung ILCs expressing IL-5, IL-13, or both IL-5 and IL-13. (H) 6-d experimental model of papain-induced airway inflammation. (I) Inflammation score from hematoxylin and eosin staining of lung sections (see Materials and methods). Note the thicker and more circumferential inflammatory infiltrates cuffing a representative 17~92$^{+/+}$ versus 17~92$^{\Delta/\Delta}$ mice bronchiole (B, top) and vessel (V, bottom). The thickness of the bronchiole or vessel wall without inflammation is highlighted by a dashed white line for reference. Bars, 40 µm. (J) qPCR quantification of IL-13–induced repair genes in epithelial brushing of papain-treated mice. Data are representative of three independent experiments each with 5–10 mice in each group (A–F). Bars represent mean ± SEM. P-values were calculated using one-way ANOVA with Sidak's multiple comparison between papain-treated 17~92$^{+/+}$ and 17~92$^{\Delta/\Delta}$ mice (B–F) or with Student's *t* test (G–J).

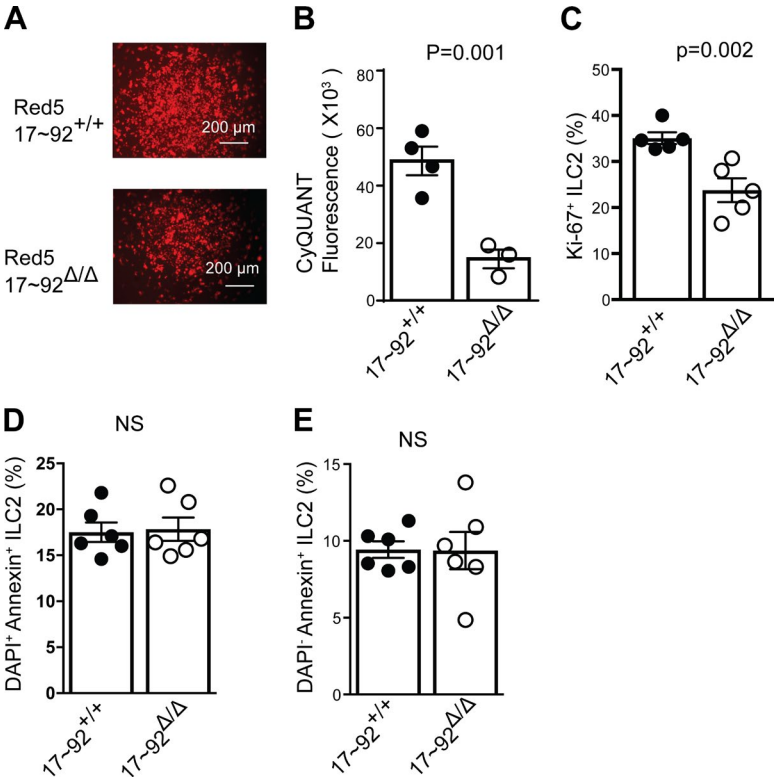

Figure 5. **The miR-17~92 cluster promotes ILC2s proliferation.** (A) Microscopic view of tdTomato fluorescence in Red5$^+$ ILC2s. Bars, 200 µm. (B) CyQUANT NF cell proliferation assay fluorescent quantification of 17~92$^{\Delta/\Delta}$ and 17~92$^{+/+}$ ILC2s after culture for 4 d. (C) Quantification of Ki67$^+$ 17~92$^{\Delta/\Delta}$ and 17~92$^{+/+}$ ILC2s frequencies after culture for 3 d. (D and E) Apoptosis in 17~92$^{\Delta/\Delta}$ and 17~92$^{+/+}$ ILC2s was assessed using Annexin V and DAPI staining on day 4 of culture. Bar graphs show the percentage of dead apoptotic ILC2s (DAPI$^+$ Annexin$^+$; D) and live apoptotic ILC2s (DAPI$^-$ Annexin$^-$; E). NS, not significant. Data in A, B, D, and E are representative of at least 20, 4, and 2 independent experiments, respectively. Bars represent mean ± SEM. P-values were calculated with Student's *t* test (B–E).

of miRNA biogenesis by inactivating Dgcr8 in *Il5*-expressing cells provoked extensive loss of ILC2s, revealing a critical role for miRNAs in ILC2 homeostasis. In addition, we identified the miRNA repertoire of resting and cytokine-activated murine ILC2s, providing critical information and a framework for formulating questions about miRNA participation in the regulatory circuits that control ILC2 biology. Consistent with their similar gene expression and cytokine production profiles (Van Dyken et al., 2016), ILC2s and T_H2 cells exhibited broadly shared miRNA repertoires. It is tempting to speculate that miRNAs expressed in both ILC2s and T_H2 cells might regulate common pathways that determine their similar immune effector phenotypes. Indeed, our analysis of miR-19 demonstrates that overlapping but nonidentical miRNA :target networks govern common functional behaviors in ILC2s and T_H2 cells.

In addition, ILC2s actively reset their miRNA repertoire when stimulated with TSLP and IL-33, similar to the behavior of T cells activated by antigen stimulation (Bronevetsky et al., 2013). This finding suggests that the post-transcriptional down-regulation of mature miRNAs and concurrent changes in primary miRNA transcription that rapidly establish a new pattern of miRNA expression in activated T cells may operate similarly downstream of cytokine signals in ILC2s. We observed this dynamic cytokine-induced change in miRNA expression in ILC2s stimulated in vitro, but very similar profiles of miRNA expression in ILC2s harvested from lungs with and without IL-33 exposure in vivo. Either IL-33 is insufficient to drive miRNA expression changes in the context of the tissue microenvironment, or miRNA expression recovers to homeostatic levels rapidly after the IL-33 source is exhausted.

A few miRNAs exhibited markedly different expression patterns in ILC2s and T_H2 cells. For example, miR-126 was abundant in ILC2s and strongly down-regulated upon cytokine activation, but scarcely expressed in naive T cells and moderately up-regulated in differentiated T_H2 cells in vitro and in vivo. Because miR-126a antagonists inhibit the response to house dust mite allergen in a mouse model of asthma (Mattes et al., 2009), these findings raise the possibility that miR-126a may be functionally important for ILC2 sentinel function in the initiation of type 2 immune responses. It is also possible that a subset of tissue-resident T_H2 cells may further modulate their expression of miR-126 and other miRNAs to more closely resemble the pattern observed in ILC2s.

The miR-17~92 cluster has many established functions in lymphocytes. It promotes the proliferation and survival of T cells and regulates the differentiation and function of several effector T cell subsets, including T_H2 cells (Xiao et al., 2008; Jiang et al., 2011; Steiner et al., 2011; Baumjohann et al., 2013; de Kouchkovsky et al., 2013; Kang et al., 2013; Simpson et al., 2014; Han et al., 2015). All six miR-17~92 cluster miRNAs were expressed similarly in ILC2s and T_H2 cells, and ILC2s lacking the cluster also exhibited defective induction of allergic inflammation in vivo and in proliferation and type 2 cytokine production in response to TSLP,

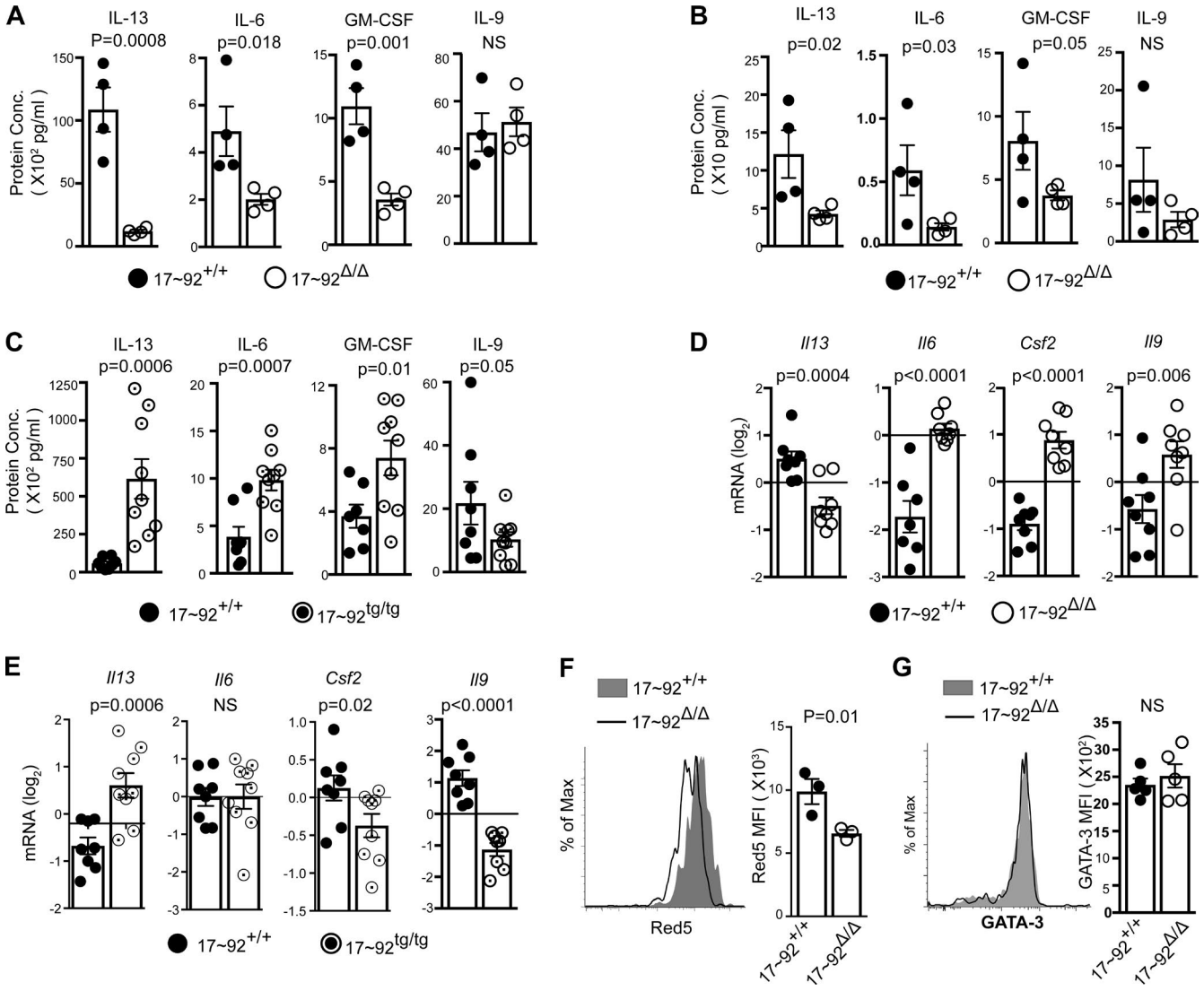

Figure 6. **The miR-17~92 cluster regulates cytokines production from ILC2s.** (A and B) IL-13, IL-6, GM-CSF, and IL-9 measured by cytometric bead array (CBA) in supernatants from 10- and 2-d cultured 17~92$^{\Delta/\Delta}$ and 17~92$^{+/+}$ ILC2s, respectively. (C) IL-13, IL-6, GM-CSF, and IL-9 measured by CBA in supernatants from 10-d cultures of 17~92$^{+/+}$ and 17~92$^{tg/tg}$ ILC2s. (D and E) Quantitative PCR quantification of *Il13*, *Il6*, *Csf3*, and *Il9* in 10-d cultured ILC2s, normalized to *Gapdh*. (F) Red5 tdTomato median fluorescence intensity (MFI) in 4-d-cultured ILC2s, assessed by flow cytometry as an indirect measure of *Il5* expression. (G) Flow cytometry analysis of GATA-3 expression in 17~92$^{\Delta/\Delta}$ and 17~92$^{+/+}$ ILC2s at day 3 of culture, presented as MFI of GATA-3 expression in live singlet. Each culture was started with 3,500 (A–F) ILC2s, sorted from an individual mouse or pools of two to three mice, and cultured with IL-33, TSLP, and IL-7. Data in A and B are representative of at least 10 independent experiments. Data in D are pooled from three independent experiments. Data in F are representative of two independent experiments. Bars represent mean ± SEM. P-values were calculated with Student's *t* test (A–G).

IL-7, and IL-33 in vitro. IL-33 is a potent activator of lung ILC2s (Bartemes et al., 2012; Kamijo et al., 2013), and the genes encoding IL-33 and its receptor ST2 are major susceptibility loci for human asthma (Moffatt et al., 2010). ST2 surface expression was normal in resting and activated 17~92$^{\Delta/\Delta}$ ILC2s. Reduced IL7R expression was observed in miR-17~92–deficient common lymphoid progenitors and thymocytes (Regelin et al., 2015). However, we observed no difference in IL7R or TSLPR expression in cultured ILC2s. Thus, modulation of signaling or gene expression downstream of these cytokine receptors must be responsible for the altered responses of 17~92$^{\Delta/\Delta}$ ILC2s.

In miR-17~92–deficient T_H2 cells, miR-19a and miR-19b restored IL-13 production, but other miRNAs of the cluster did not (Simpson et al., 2014). miR-19a also restored IL-13 production in 17~92$^{\Delta/\Delta}$ ILC2s. We identified two important pieces of the miR-19 target network in ILC2s: *Tnfaip3* and *Socs1*. Both of these targets encode inhibitors of cytokine signaling pathways, indicating that miR-19 supports the production of IL-13 and IL-5 by simultaneously amplifying signals

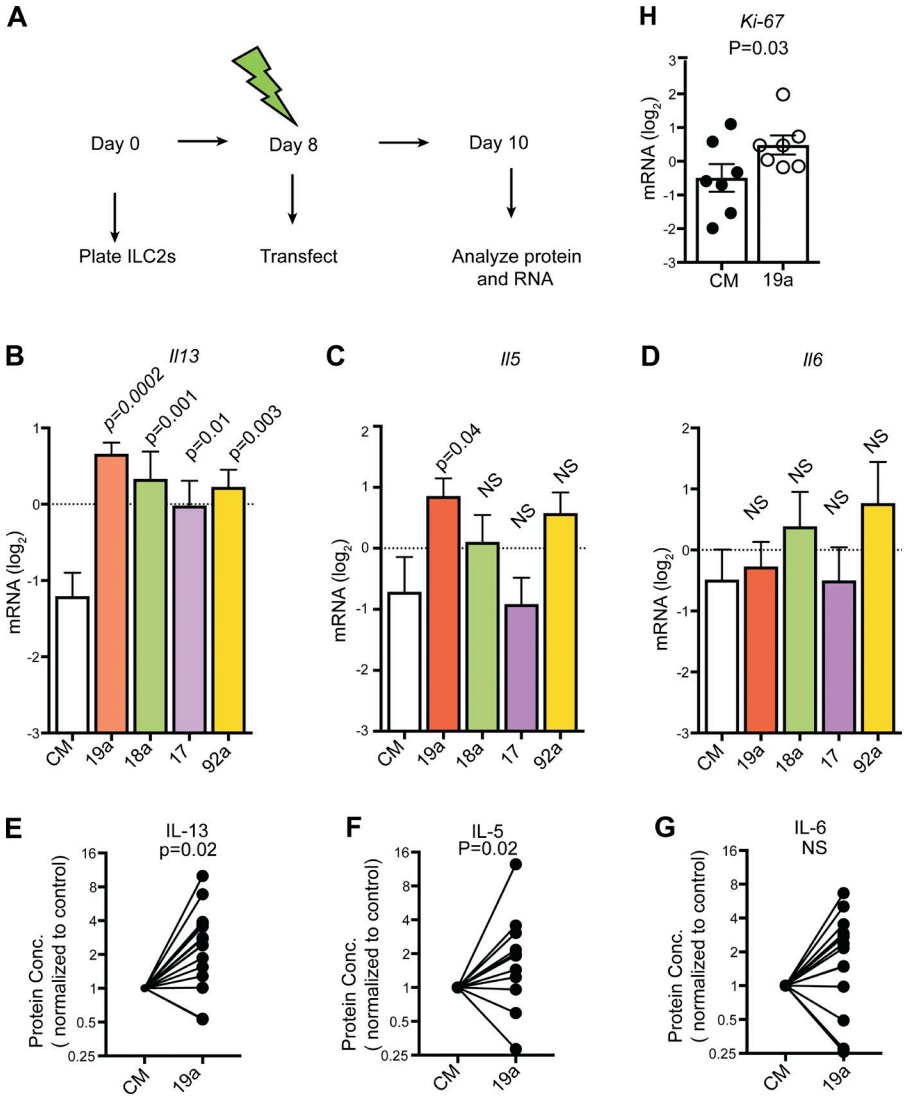

Figure 7. **Cell-intrinsic defect in IL-13 and IL-5 production in 17∼92$^{\Delta/\Delta}$ ILC2s rescued by miR-19a.** (A) 10-d experimental model of next-generation transfection of ILC2s. Each culture was started with 10,000–12,000 17∼92$^{\Delta/\Delta}$ ILC2s sorted from the pool of three to six mice and cultured with IL-33, TSLP, and IL-7. Cells were transfected on day 8 with control mimic (CM) or mimics of miR-19a, miR-18a, miR-17, and miR-92a and harvested on day 10. (B–D) Quantitative PCR (qPCR) quantification of *Gapdh*-normalized *Il13*, *Il5*, and *Il6* mRNA from 17∼92$^{\Delta/\Delta}$ ILC2s transfected with CM or miR-19a, miR-18a, miR-17, and miR-92a mimic. (E–G) IL-13, IL-5, and IL-6 measured by cytometric bead array (CBA) in supernatants from 17∼92$^{\Delta/\Delta}$ ILC2s transfected with miR-19a or control miRNA mimic. Data are pooled from five independent experiments and are normalized to matched control mimic transfection in each biological replicate. Bars represent mean ± SEM. (H) qPCR quantification of *Gapdh*-normalized *Ki-67* mRNA expression from 17∼92$^{\Delta/\Delta}$ ILC2s transfected with miR-19a or control miRNA mimic. Bars represent mean ± SEM. Data in B–D and H are pooled from two independent experiments. P-values were calculated with one-way ANOVA with Dunnett's multiple comparison post hoc test (comparing each column to CM; B–D), paired Student's *t* test on unnormalized data (E–G), or Student's *t* test (H).

downstream of IL-33 and IL-7/TSLP. *Tnfaip3* encodes A20, a powerful negative regulator of the NF-κB pathway previously identified as an important target of miR-19 in macrophages and T_H2 cells (Gantier et al., 2012; Simpson et al., 2014). SOCS1 inhibits the JAK-STAT pathway downstream of IL-7 and other related cytokines, and also limits type 2 cytokine production in T_H2 cells (Simpson et al., 2014). Our analysis in ILC2s revealed a limiting role for both of these miR-19 target genes, as depleting each individually with siRNAs was sufficient to markedly increase IL-13 and IL-5 production. These findings suggest that both A20 and SOCS1 are important miR-19 targets that regulate the ILC2 effector function. Genome-wide approaches to determine the full miR-19 target network in ILC2s would probably reveal additional targets involved in ILC2 biology.

The tumor suppressor *Pten* is another important miR-19 target that has been implicated in miRNA control of many biological processes (Baumjohann and Ansel, 2013). However, *Pten* expression was unaltered by miR-17∼92 deficiency or miR-19a mimic transfection into ILC2s. Genetic rescue of the *Pten* overexpression observed in miR-17∼92–deficient T_H2 cells partially restored IL-13 production (Simpson et al., 2014), but apparently this mode of regulation is not operational in ILC2s. In contrast, two miR-19 targets that are not highly expressed in T_H2 cells were regulated by miR-19 in ILC2s: *Kit* and *Rora*. c-Kit is a receptor tyrosine kinase often used to identify mouse and human ILC2 cells. *Rora* is a direct target of multiple miR-17∼92 cluster miRNAs, and aberrant expression of the transcription factor that it encodes, RORα, disrupts the fidelity of lineage-specific gene expression in miR-17∼92–deficient follicular helper T cells (Baumjohann et al., 2013). RORα is critical for ILC2 development, but little is known about its contribution to functional aspects of ILC2 biology (Wong et al., 2012). Polymorphisms in the human *RORA* locus are associated with asthma susceptibility (Moffatt et al., 2010). Future studies may uncover additional functionally relevant miR-17∼92 targets in ILC2s.

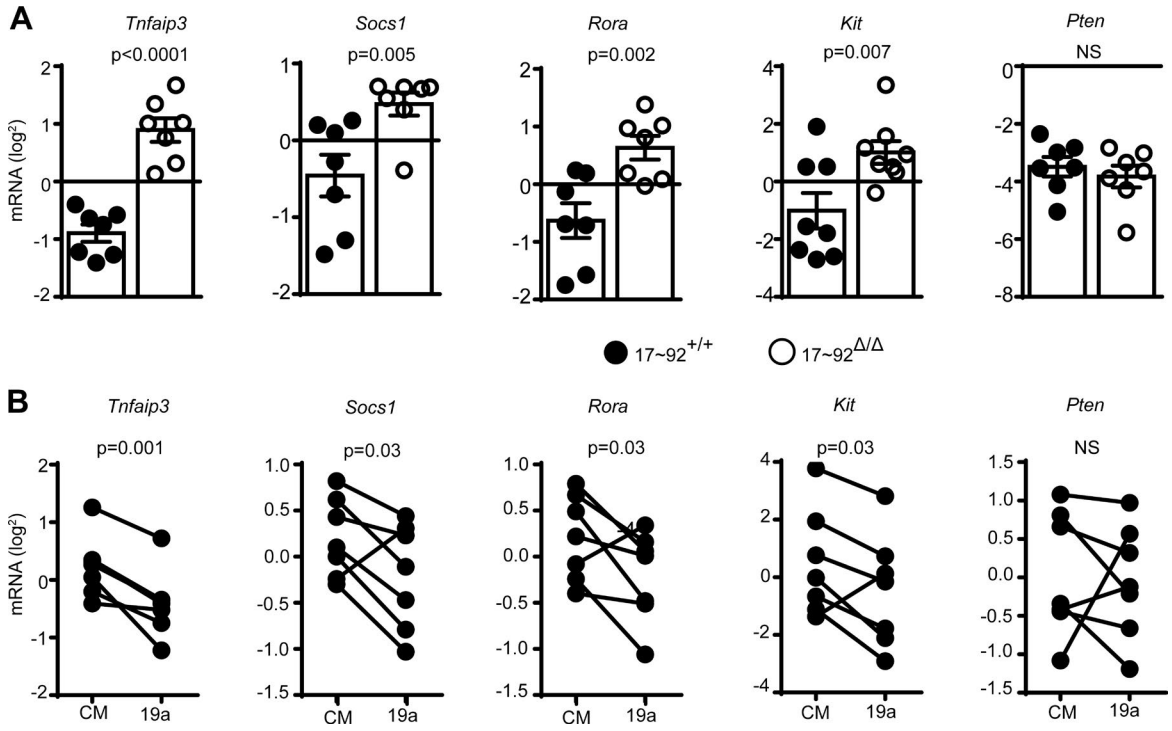

Figure 8. **miR-19 regulates target gene expression in ILC2s.** (A) Quantitative PCR (qPCR) quantification of the indicated candidate miR-19a target mRNAs in 10-d-cultured 17~92$^{+/+}$ and 17~92$^{\Delta/\Delta}$ ILC2s. (B) qPCR quantification of mRNAs in 17~92$^{\Delta/\Delta}$ ILC2s transfected with control mimic (CM) or miR-19a mimic (19a). Data are normalized to *Gapdh* mRNA. Each culture was started with 3,500 (A) or 10,000 (B) ILCs, sorted from pools of two to six mice. Data are pooled from three independent experiments (A and B). Bars represent mean ± SEM. P-values were calculated with Student's *t* test (A) or paired Student's *t* test (B).

In addition to augmenting IL-13 and IL-5 production, miR-17~92 surprisingly reduced ILC2 expression of *Il9*, *Il6*, and *Csf2* (GM-CSF). These latter effects were not rescued by transfection with mimics corresponding to each miRNA family in the miR-17~92 cluster, although transgenic overexpression of the entire cluster reduced *Il9* and *Csf3* expression. These findings verify that 17~92$^{\Delta/\Delta}$ ILC2s are capable of efficient cytokine production and highlight the specificity of miR-19 regulation of IL-13 and IL-5. In addition, they suggest that multiple miR-17~92 miRNAs act in concert to coordinate regulatory networks that control ILC2 cytokine production and expansion in response to IL-33.

In conclusion, this study provides concrete evidence that miRNAs regulate diverse aspects of ILC2 biology. Using mouse genetic tools and a novel protocol for ILC2 transfection with siRNAs and miRNA mimics, we dissected the mechanism by which the miR-17~92 cluster regulates type 2 cytokine production. miR-19a regulates IL-13 production through overlapping but nonidentical downstream target networks in ILC2s and T_H2 cells, suggesting that miR-19a itself might be an attractive therapeutic target (Lu and Rothenberg, 2013). Alternatively, targeting the same signaling pathways modulated by miR-19 could be an effective intervention for asthma and allergic diseases (Edwards et al., 2009). Our findings open new avenues for understanding the gene expression programs and signaling pathways that underlie the onset of allergic responses by innate and adaptive lymphocytes.

MATERIALS AND METHODS

Mice

Mice with *loxP*-flanked alleles encoding miR-17~92 (*Mirc1*$^{fl/fl}$, 008458; The Jackson Laboratory) and Rosa26-Mir-17~92-transgenic mice Gt(ROSA)26Sor$^{tm3(CAG-MIR17-92,-EGFP)RSKY}$, 008517; The Jackson Laboratory) were crossed to *Il5*$^{tm1.1(cre)LKy}$ (Red5) mice (Nussbaum et al., 2013) to delete the floxed alleles specifically in IL-5–producing cells. *Dgcr8*$^{tm1.1Blel}$ (*Dgcr8*$^{fl/fl}$); Gt(ROSA)26Sor$^{tm3(CAG-EYFP)Hze}$ (Rosa-YFP; Rao et al., 2009) were provided by R. Blelloch (University of California, San Francisco) and crossed with Red5 mice to generate Red5 Dgcr8$^{fl/fl}$ ROSA-YFP mice (here *Dgcr8*$^{\Delta/\Delta}$). *Il4*^{tm1LKy} (4get) mice have been described previously (Mohrs et al., 2001). Male and female mice used were 5–9 wks of age on the C57BL/6 background (≥10 backcross generations). All mice were housed and bred in the specific pathogen–free barrier facility at the University of California, San Francisco. The Institutional Animal Care and Use Committee at the University of California, San Francisco, approved all animal experiments.

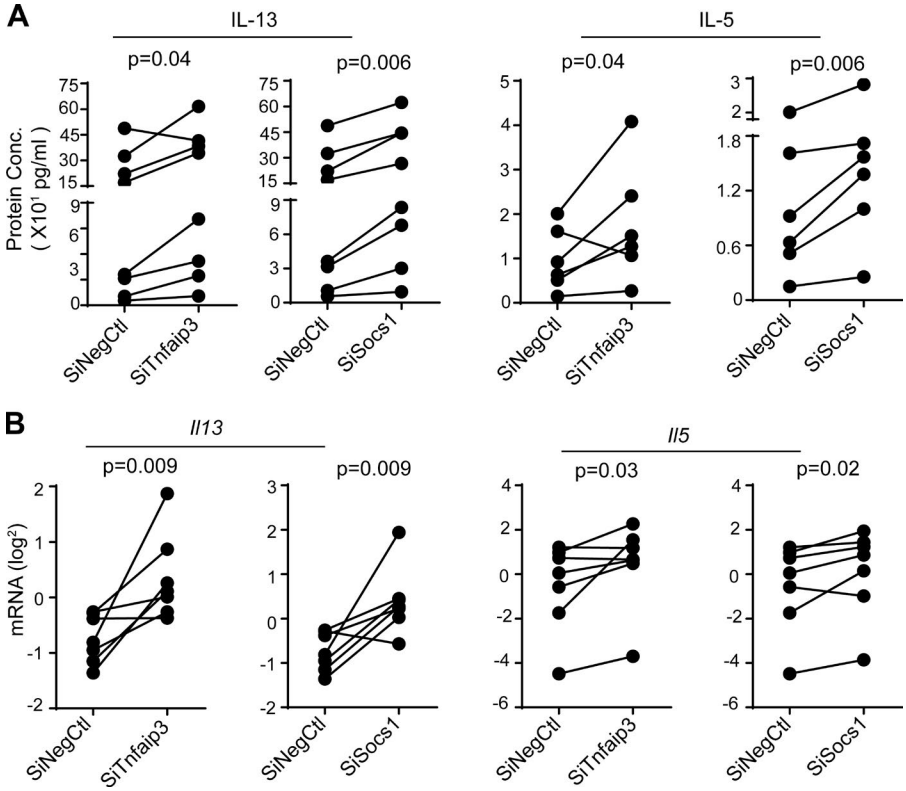

Figure 9. **miR-19 targets *Tnfaip3* and *Socs1* negatively regulate IL-13 and IL-5 expression in ILC2s.** (A) IL-13 and IL-5 measured by cytometric bead array (CBA) in supernatants from $17{\sim}92^{\Delta/\Delta}$ ILC2s transfected with siRNAs targeting *Tnfaip3* or *Socs1* or negative control siRNA (siNegCtl). (B) Quantitative PCR quantification of *Il13* and *Il5* mRNA, normalized to *Gapdh* mRNA. Each culture was started with 10,000 ILC2s sorted from pools of five to seven mice. Data are pooled from three independent experiments. P-values were calculated with paired Student's *t* test.

Lung digestion

For flow cytometric analysis or sorting of ILC2s, lungs were perfused with PBS via the right ventricle until it blanched. Lung lobes were excised and processed with a gentleMACS automated tissue dissociator in C tubes (Miltenyi Biotec), running program "m_lung_01," followed by shaking incubation for 35 min at 37°C, 175 rpm, in RPMI medium containing 50 µg/ml Liberase TM and 25 µg/ml DNAs1 (Roche). After incubation, a second dissociation was performed with program "m_lung_02." After tissue dissociation, cell suspensions were filtered through a 70-µm nylon mesh, washed, and treated with BD Pharm Lyse lysing solution (BD Biosciences) to lyse red blood cells before final suspension in PBS with 3% FBS.

Flow cytometry and sorting

Monoclonal, murine-specific antibodies from BioLegend included anti-B220 (RA3-6B2), anti–Gr-1 (RB6-8C5), anti-F4/80 (BM8), anti-CD3 (145-2C11), anti-CD49b (DX5), anti-NK1.1 (PK136), anti-CD4 (RM4-5), anti-CD11c (N418), anti-CD4 (GK 1.5), anti-CD8a (53–6.7), and anti–IL-5 (TRFK5). Antibodies from eBioscience included anti-CD25 (PC61.5), anti-CD90.2 (53–2.1), anti-CD4 (GK1.5), anti-CD4 (RM4.5), anti-CD11b (M1/70), and anti–Ly-6G (RB6-8C5). Antibodies from BD Biosciences included anti-CD11C (HL3), Streptavidin, anti-CD45 (30-F11), anti–Siglec-F (E50-2440), anti-Ki67 (SolAI5), anti–IL-13 (eBio13A), and anti-GATA3 (TWAJ). Antibodies from TONBO Biosciences included anti-CD11b (M1/70). Nonspecific antibody binding was blocked with anti-CD16/CD32 plus 2% normal mouse/rat serum. Dead cells were excluded with Fixable Viability Dye eFluor780 (eBioscience). Sample data were acquired with a LSRII flow cytometer (BD Biosciences) and analyzed using FlowJo software. Cells were sorted using a FACS Aria II (Beckman Coulter).

For measurement of intracellular cytokine expression, cells were isolated ex vivo and stimulated in complete high-glucose DMEM supplemented with 10% heat-inactivated FBS, penicillin/streptomycin/L-glutamine, 2-mercaptoethanol with 50 ng/ml phorbol 12-myristate 13-acetate (Sigma-Aldrich), 500 ng/ml ionomycin (Sigma-Aldrich), and 10 µg/ml brefeldin A (Sigma-Aldrich) for 4 h. Cells were stained with the viability dye eFluor780 and fixed in 4% PFA for 8 min at room temperature. Cytokine staining was done in permeabilization buffer containing 0.5% saponin (Invitrogen). For analysis of transcription factor expression, cultured cells were fixed and permeabilized according to the manufacturer's instructions (Foxp3/Transcription Factor Staining Buffer Set; eBioscience).

In vitro cultures and transfection

Sorted ILC2s were cultured (37°C, 10% CO_2) at 3,000–10,000 cells per well in 200 µl high-glucose DMEM supplemented with 10% heat-inactivated FBS, penicillin/streptomycin/L-glutamine, 2-mercaptoethanol, recombinant mouse cytokines, IL-33, TSLP, and IL-7 at 10 ng/ml (R&D

Systems). At harvest, cell-free culture supernatants were collected, and cells were analyzed by flow cytometry or collected in TRIzol LS (Thermo Fisher Scientific) for RNA extraction. On day 8 of culture, ILC2s were transfected with miRNA mimics and siRNAs (Dharmacon). miRIDIAN miRNA mimics were used at 500 nM per transfection. siGENOME SmartPools and ON-TARGETplus Individual siRNAs were used at 500 nM. Cells were transfected using the Neon Transfection system (Invitrogen) as previously described (Steiner et al., 2011). Cells and culture supernatants were harvested on day 10 for further analysis.

CyQUANT NF cell proliferation assay

CyQUANT NF Cell Proliferation Assay kit (Thermo Fisher Scientific) was used to measure proliferation of 4-d-cultured ILC2s, which were analyzed on a FLUOstar Optima plate reader (BMG Labtech).

Cytokine protein analysis

For ILC2 culture supernatants and BAL, IL-13, IL-5, IL-9, IL-6, and GM-CSF were quantified by cytometric bead array using a LSRII flow cytometer and FCAP Array analysis software (BD Biosciences).

RNA isolation and quantitative RT-PCR

ILC2s, $CD4^+$ T cells, and T_H2 cells were sorted directly into TRIzol LS (Thermo Fisher Scientific). Cultured ILC2s, T_H2 cells, or gentleMACS-homogenized lung cells were also frozen in TRIzol LS (Thermo Fisher Scientific), and RNA was isolated using the miRNeasy Micro kit (Qiagen). RNA was reverse-transcribed with the SuperScript III kit (Invitrogen). Primers used for SYBR Green PCRs are as follows: *Gapdh*: 5′-GTGTTCCTACCCCCAATGTGT-3′, 5′-ATTGTCATACCAGGAAATGAGCTT-3′; *Il9*: 5′-ATGTTGGTGACATACATCCTTGC-3′, 5′-TGACGGTGGATCATCCTTCAG-3′; *Il5*: 5′-CTCTGTTGACAAGCAATGAGACG-3′, 5′-TCTTCAGTATGTCTAGCCCCTG-3′; *Il13*: 5′-CCTGGCTCTTGCTTGCCTT-3′, 5′-GGTCTTGTGTGATGTTGCTCA-3′; *Csf2*: 5′-GTCTCTAACGAGTTCTCCTTC A-3′, 5′-CCTTGAGTTTGGTGAAATTGCC-3′; *Il6*: 5′-AGCCAGAGTCCTTCAGAGA-3′, 5′-TCCTTAGCCACTCCTTCTGT-3′; *Rora*: 5′-CTTCTCGGTGGTTCTTCTGT-3′, 5′-TTCTGCATTCGTACTGATGTCA-3′; *Socs-1*: 5′-ATTCCACTCCTACCTCTCCAT-3′, 5′-CAGAAAAATGAAGCCAGAGACC-3′; *Tnfaip3*: 5′-AGAACCAGAGATTCCATGAAGC-3′, 5′-CTGTGTAGTTCGAGGCATGT-3′; *Kit*: 5′-CCATAGGACCAGACATCACTT-3′, 5′-CTAGCCAGAGACATCAGGAATG-3′; *Pten*: 5′ TAATATACATAGCGCCTCTGACTG-3′, 5′-CGGACTGGTGTAATGATTTGTG-3′; *Muc5ac*: 5′-CAGGACTCTCTGAAATCGTACCA-3′, 5′-AAGGCTCGTACCACAGGGA-3′; *Clca3*: 5′-CTGTCTTCCTCTTGATCCTCCA-3′, 5′-CGTGGTCTATGGCGATGACG-3′; and *Gob5*: 5′-CATCGCCATAGACCACGACG-3′, 5′-TTCCAGCTCTCGGGAATCAAA-3′.

In vivo allergic inflammation model

Mice were anesthetized using isoflurane inhalation and challenged with 35 µg papain (Calbiochem) in 40 µl PBS administered to the lungs by oropharyngeal aspiration daily for three consecutive days. Samples were harvested on day 4. BAL was performed by three consecutive washes of 1 ml complete medium. The number of cells in BAL and lung samples was quantified by FACS analysis with AccuCount Particles (Spherotech). For lung pathology, mice were challenged with 35 µg papain in 40 µl PBS on days 1, 3, and 5, and samples were harvested on day 6. A blinded pathologist scored inflammation in lungs on day 6 using routine hematoxylin and eosin–stained paraffin sections. Both the right and left lungs were examined. Perivascular, peribronchiolar, and interstitial/alveolar inflammation was scored for percentage involvement (0% = 0, 1–25% = 1, 26–50% = 2, 51–75% = 3, and 76–100% = 4). Perivascular and peribronchiolar inflammation was also scored for the mean thickness of the inflammatory cuff (0 cells = 0, 1–3 cells = 1, and ≥4 cells = 2). The values were summed for each sample to determine the inflammation score. One mouse was excluded because of histological evidence of acute bronchopneumonia, and two mice were excluded for a paucity of bronchioles available for evaluation.

Small RNA sequencing

5–50 ng total RNA from sorted and/or cultured ILC2 and T cell samples were used to build small RNA libraries as previously described (Williams et al., 2013). Libraries were sequenced on a HiSeq2500 (Illumina). Data were demultiplexed and adapters trimmed using the FastX Toolkit (http://hannonlab.cshl.edu/fastx_toolkit/index.html). Sequence alignment and small RNA read counts were obtained using the exceRpt small RNA-seq Pipeline (v3; https://www.genboree.org/epigenomeatlas/genboreeWorkbench.rhtml). Comparative expression analysis was performed with DESeq2 (Love et al., 2014). Raw RNA sequencing data were deposited in the GEO database (GSE96934). Three or four biological replicates were collected for each cell type and condition. ILC2 cells were sorted from the lungs of control mice (ILC2) or the lungs of mice killed 1 d after treatment for three consecutive days with 500 ng IL-33 (R&D Systems) instilled by oropharyngeal aspiration (ILC2 IL33). Sorted ILC2s from control mice were also cultured in vitro for 10 d with 10 ng/ml IL-33, TSLP, and IL-7 from R&D Systems (ILC2 in vitro). Naive $CD4^+$ T cells were sorted from pooled spleen and lymph nodes of control mice (CD4). T_H2 cells were generated in vitro under polarizing conditions including 500 U/ml IL-4 supernatant and anti-IFNγ (T_H2 in vitro) as described (Pua et al., 2016). An in vivo population of T_H2 cells was generated by the induction of AA responses to OVA as previously described (Pua et al., 2016), with slight modification: 4get mice were sensitized with three weekly i.p. injections of OVA-alum and challenged with OVA in the lung for three consecutive days by oropharyngeal aspiration, and $CD4^+GFP^+$ T_H2 cells were then sorted from BAL fluid 1 d after the final challenge (T_H2 AA).

For ILC2, ILC2 IL33, CD4, and T_H2 AA, 8,000–1,000,000 cells were sorted on either FACSAria II or FACSAria IIIu (BD Biosciences) directly into TRIzol LS (Thermo Fisher Scientific). For sorting, the following gating strategies were used: ILC2, ILC2 IL33, and ILC2 in vitro: $CD45^+Thy1^+lin^-CD4^-CD25^+ST2^+$; CD4: $CD4^+CD62L^{hi}CD44^{lo}CD25^-CD69^-$; and T_H2 AA: $CD45^+CD11c^-CD11b^-CD4^+CD3^+4get^+$. For ILC2 in vitro, 10,000 sorted cells were seeded into wells, and the entire cell population was lysed in TRIzol LS after 10 d of culture. For T_H2 in vitro, 3,000,000 cells were collected from T_H2-polarizing cultures at day 5 and lysed with TRIzol LS. Total RNA was isolated using a miRNeasy Micro kit (Qiagen), and RNA was quantified using an RNA Pico kit on the Bioanalyzer (Agilent).

Statistical analysis

Excel (Microsoft) and Prism (Graph Pad Software) were used for data analysis. Unless otherwise specified, p-values were calculated using unpaired Student's *t* tests. For comparisons of multiple groups, ANOVA was used with appropriate post hoc testing.

Online supplemental material

Table S1 summarizes mapped reads for small RNA sequencing of ILC2s and T cells. Table S2 details differential expression analyses for all pairwise comparisons of ILC2, ILC2 IL33, ILC2 in vitro, CD4, T_H2 AA, and T_H2 small RNA sequencing miRNA expression data. Table S3 lists miRNAs in groups of hierarchically clustered rows from differential expression analysis of small RNA sequencing data in ILC2 and T cell samples. Table S4 provides DESeq2 normalized miRNA expression for ILC2 and T cell samples. Tables S1–S4 are provided as zipped Excel files.

ACKNOWLEDGMENTS

All sequencing was performed at the Center for Advanced Technology at the University of California, San Francisco, and the Vincent J. Coates Genomic Sequencing Laboratory at the University of California, Berkeley. We thank Vinh Nguyen for his assistance in ILC2 sorts.

This work was supported by US National Institutes of Health grants (R01HL109102, P01HL107202, and U19CA179512); a Leukemia and Lymphoma Society Scholar award (K.M. Ansel); the National Multiple Sclerosis Society; the University of California, San Francisco Program for Breakthrough Biomedical Research, funded in part by the Sandler Foundation; and the Emmy Noether Program (BA 5132/1-1) of the Deutsche Forschungsgemeinschaft (D. Baumjohann).

The authors declare no competing financial interests.

Author contributions: P.B. Singh designed, performed, and analyzed most of the experiments; H.H. Pua analyzed RNAseq and histology data; and H.C. Happ helped to perform in vivo experiments. C. Schneider, J. von Moltke, R.M. Locksley, and D. Baumjohann helped design and interpret some experiments. D. Baumjohann and K.M. Ansel initiated the project. K.M. Ansel helped design, analyze and interpret all experiments. P.B. Singh and K.M. Ansel wrote the manuscript. All authors reviewed and approved the manuscript.

Submitted: 24 March 2017

Revised: 5 July 2017

Accepted: 21 September 2017

REFERENCES

Bartemes, K.R., K. Iijima, T. Kobayashi, G.M. Kephart, A.N. McKenzie, and H. Kita. 2012. IL-33-responsive $Lineage^-CD25^+CD44^{hi}$ lymphoid cells mediate innate type-2 immunity and allergic inflammation in the lungs. *J. Immunol.* 188:1503–1513. https://doi.org/10.4049/jimmunol.1102832

Baumjohann, D., and K.M. Ansel. 2013. MicroRNA-mediated regulation of T helper cell differentiation and plasticity. *Nat. Rev. Immunol.* 13:666–678. https://doi.org/10.1038/nri3494

Baumjohann, D., R. Kageyama, J.M. Clingan, M.M. Morar, S. Patel, D. de Kouchkovsky, O. Bannard, J.A. Bluestone, M. Matloubian, K.M. Ansel, and L.T. Jeker. 2013. The microRNA cluster miR-17~92 promotes TFH cell differentiation and represses subset-inappropriate gene expression. *Nat. Immunol.* 14:840–848. https://doi.org/10.1038/ni.2642

Beaulieu, A.M., N.A. Bezman, J.E. Lee, M. Matloubian, J.C. Sun, and L.L. Lanier. 2013. MicroRNA function in NK-cell biology. *Immunol. Rev.* 253:40–52. https://doi.org/10.1111/imr.12045

Bronevetsky, Y., A.V. Villarino, C.J. Eisley, R. Barbeau, A.J. Barczak, G.A. Heinz, E. Kremmer, V. Heissmeyer, M.T. McManus, D.J. Erle, et al. 2013. T cell activation induces proteasomal degradation of Argonaute and rapid remodeling of the microRNA repertoire. *J. Exp. Med.* 210:417–432. https://doi.org/10.1084/jem.20111717

Christianson, C.A., N.P. Goplen, I. Zafar, C. Irvin, J.T. Good Jr., D.R. Rollins, B. Gorentla, W. Liu, M.M. Gorska, H. Chu, et al. 2015. Persistence of asthma requires multiple feedback circuits involving type 2 innate lymphoid cells and IL-33. *J. Allergy Clin. Immunol.* 136:59–68.e14. https://doi.org/10.1016/j.jaci.2014.11.037

Curtale, G., F. Citarella, C. Carissimi, M. Goldoni, N. Carucci, V. Fulci, D. Franceschini, F. Meloni, V. Barnaba, and G. Macino. 2010. An emerging player in the adaptive immune response: microRNA-146a is a modulator of IL-2 expression and activation-induced cell death in T lymphocytes. *Blood.* 115:265–273. https://doi.org/10.1182/blood-2009-06-225987

de Kouchkovsky, D., J.H. Esensten, W.L. Rosenthal, M.M. Morar, J.A. Bluestone, and L.T. Jeker. 2013. microRNA-17-92 regulates IL-10 production by regulatory T cells and control of experimental autoimmune encephalomyelitis. *J. Immunol.* 191:1594–1605. https://doi.org/10.4049/jimmunol.1203567

Deshpande, D.A., M. Dileepan, T.F. Walseth, S. Subramanian, and M.S. Kannan. 2015. MicroRNA regulation of airway inflammation and airway smooth muscle function: Relevance to asthma. *Drug Dev. Res.* 76:286–295. https://doi.org/10.1002/ddr.21267

de Yébenes, V.G., N. Bartolomé-Izquierdo, and A.R. Ramiro. 2013. Regulation of B-cell development and function by microRNAs. *Immunol. Rev.* 253:25–39. https://doi.org/10.1111/imr.12046

Diefenbach, A., M. Colonna, and S. Koyasu. 2014. Development, differentiation, and diversity of innate lymphoid cells. *Immunity.* 41:354–365. https://doi.org/10.1016/j.immuni.2014.09.005

Edwards, M.R., N.W. Bartlett, D. Clarke, M. Birrell, M. Belvisi, and S.L. Johnston. 2009. Targeting the NF-kappaB pathway in asthma and chronic obstructive pulmonary disease. *Pharmacol. Ther.* 121:1–13. https://doi.org/10.1016/j.pharmthera.2008.09.003

Fehniger, T.A., T. Wylie, E. Germino, J.W. Leong, V.J. Magrini, S. Koul, C.R. Keppel, S.E. Schneider, D.C. Koboldt, R.P. Sullivan, et al. 2010. Next-generation sequencing identifies the natural killer cell microRNA transcriptome. *Genome Res.* 20:1590–1604. https://doi.org/10.1101/gr.107995.110

Gantier, M.P., H.J. Stunden, C.E. McCoy, M.A. Behlke, D. Wang, M. Kaparakis-Liaskos, S.T. Sarvestani, Y.H. Yang, D. Xu, S.C. Corr, et al. 2012. A miR-19 regulon that controls NF-κB signaling. *Nucleic Acids Res.* 40:8048–8058. https://doi.org/10.1093/nar/gks521

Gordon, E.D., L.J. Simpson, C.L. Rios, L. Ringel, M.E. Lachowicz-Scroggins, M.C. Peters, A. Wesolowska-Anderson, J.R. Gonzalez, H.J. MacLeod, L.S. Christian, et al. 2016. Alternative splicing of interleukin-33 and type

2 inflammation in asthma. *Proc. Natl. Acad. Sci. USA.* 113:8765–8770. https://doi.org/10.1073/pnas.1601914113

Han, Y.-C., J.A. Vidigal, P. Mu, E. Yao, I. Singh, A.J. González, C.P. Concepcion, C. Bonetti, P. Ogrodowski, B. Carver, et al. 2015. An allelic series of miR-17 ~ 92-mutant mice uncovers functional specialization and cooperation among members of a microRNA polycistron. *Nat. Genet.* 47:766–775. https://doi.org/10.1038/ng.3321

Hsu, S.-D., F.-M. Lin, W.-Y. Wu, C. Liang, W.-C. Huang, W.-L. Chan, W.T. Tsai, G.Z. Chen, C.J. Lee, C.M. Chiu, et al. 2011. miRTarBase: A database curates experimentally validated microRNA-target interactions. *Nucleic Acids Res.* 39(suppl_1):D163–D169. https://doi.org/10.1093/nar/gkq1107

Jiang, S., C. Li, V. Olive, E. Lykken, F. Feng, J. Sevilla, Y. Wan, L. He, and Q.J. Li. 2011. Molecular dissection of the miR-17-92 cluster's critical dual roles in promoting Th1 responses and preventing inducible Treg differentiation. *Blood.* 118:5487–5497. https://doi.org/10.1182/blood-2011-05-355644

Johansson, K., C. Malmhäll, P. Ramos-Ramírez, and M. Rådinger. 2017. MicroRNA-155 is a critical regulator of type 2 innate lymphoid cells and IL-33 signaling in experimental models of allergic airway inflammation. *J. Allergy Clin. Immunol.* 139:1007–1016.e9. https://doi.org/10.1016/j.jaci.2016.06.035

Kamijo, S., H. Takeda, T. Tokura, M. Suzuki, K. Inui, M. Hara, H. Matsuda, A. Matsuda, K. Oboki, T. Ohno, et al. 2013. IL-33-mediated innate response and adaptive immune cells contribute to maximum responses of protease allergen-induced allergic airway inflammation. *J. Immunol.* 190:4489–4499. https://doi.org/10.4049/jimmunol.1201212

Kang, S.G., W.-H. Liu, P. Lu, H.Y. Jin, H.W. Lim, J. Shepherd, D. Fremgen, E. Verdin, M.B. Oldstone, H. Qi, et al. 2013. MicroRNAs of the miR-17∼92 family are critical regulators of T(FH) differentiation. *Nat. Immunol.* 14:849–857. https://doi.org/10.1038/ni.2648

Klose, C.S.N., and D. Artis. 2016. Innate lymphoid cells as regulators of immunity, inflammation and tissue homeostasis. *Nat. Immunol.* 17:765–774. https://doi.org/10.1038/ni.3489

Kuperman, D.A., X. Huang, L.L. Koth, G.H. Chang, G.M. Dolganov, Z. Zhu, J.A. Elias, D. Sheppard, and D.J. Erle. 2002. Direct effects of interleukin-13 on epithelial cells cause airway hyperreactivity and mucus overproduction in asthma. *Nat. Med.* 8:885–889. https://doi.org/10.1038/nm734

Love, M.I., W. Huber, and S. Anders. 2014. Moderated estimation of fold change and dispersion for RNA-seq data with DESeq2. *Genome Biol.* 15:550. https://doi.org/10.1186/s13059-014-0550-8

Lu, T.X., and M.E. Rothenberg. 2013. Diagnostic, functional, and therapeutic roles of microRNA in allergic diseases. *J. Allergy Clin. Immunol.* 132:3–13, quiz :14. https://doi.org/10.1016/j.jaci.2013.04.039

Luche, H., O. Weber, T. Nageswara Rao, C. Blum, and H.J. Fehling. 2007. Faithful activation of an extra-bright red fluorescent protein in "knock-in" Cre-reporter mice ideally suited for lineage tracing studies. *Eur. J. Immunol.* 37:43–53. https://doi.org/10.1002/eji.200636745

Martinez-Gonzalez, I., C.A. Steer, and F. Takei. 2015. Lung ILC2s link innate and adaptive responses in allergic inflammation. *Trends Immunol.* 36:189–195. https://doi.org/10.1016/j.it.2015.01.005

Mattes, J., A. Collison, M. Plank, S. Phipps, and P.S. Foster. 2009. Antagonism of microRNA-126 suppresses the effector function of TH2 cells and the development of allergic airways disease. *Proc. Natl. Acad. Sci. USA.* 106:18704–18709. https://doi.org/10.1073/pnas.0905063106

Moffatt, M.F., I.G. Gut, F. Demenais, D.P. Strachan, E. Bouzigon, S. Heath, E. von Mutius, M. Farrall, M. Lathrop, and W.O.C.M. Cookson. GABRIEL Consortium. 2010. A large-scale, consortium-based genomewide association study of asthma. *N. Engl. J. Med.* 363:1211–1221. https://doi.org/10.1056/NEJMoa0906312

Mogilyansky, E., and I. Rigoutsos. 2013. The miR-17/92 cluster: A comprehensive update on its genomics, genetics, functions and increasingly important and numerous roles in health and disease. *Cell Death Differ.* 20:1603–1614. https://doi.org/10.1038/cdd.2013.125

Mohrs, M., K. Shinkai, K. Mohrs, and R.M. Locksley. 2001. Analysis of type 2 immunity in vivo with a bicistronic IL-4 reporter. *Immunity.* 15:303–311. https://doi.org/10.1016/S1074-7613(01)00186-8

Monticelli, S., K.M. Ansel, C. Xiao, N.D. Socci, A.M. Krichevsky, T.H. Thai, N. Rajewsky, D.S. Marks, C. Sander, K. Rajewsky, et al. 2005. MicroRNA profiling of the murine hematopoietic system. *Genome Biol.* 6:R71. https://doi.org/10.1186/gb-2005-6-8-r71

Nussbaum, J.C., S.J. Van Dyken, J. von Moltke, L.E. Cheng, A. Mohapatra, A.B. Molofsky, E.E. Thornton, M.F. Krummel, A. Chawla, H.E. Liang, and R.M. Locksley. 2013. Type 2 innate lymphoid cells control eosinophil homeostasis. *Nature.* 502:245–248. https://doi.org/10.1038/nature12526

Okoye, I.S., S. Czieso, E. Ktistaki, K. Roderick, S.M. Coomes, V.S. Pelly, Y. Kannan, J. Perez-Lloret, J.L. Zhao, D. Baltimore, et al. 2014. Transcriptomics identified a critical role for Th2 cell-intrinsic miR-155 in mediating allergy and antihelminth immunity. *Proc. Natl. Acad. Sci. USA.* 111:E3081–E3090. https://doi.org/10.1073/pnas.1406322111

Pua, H.H., and K.M. Ansel. 2015. MicroRNA regulation of allergic inflammation and asthma. *Curr. Opin. Immunol.* 36:101–108. https://doi.org/10.1016/j.coi.2015.07.006

Pua, H.H., D.F. Steiner, S. Patel, J.R. Gonzalez, J.F. Ortiz-Carpena, R. Kageyama, N.T. Chiou, A. Gallman, D. de Kouchkovsky, L.T. Jeker, et al. 2016. MicroRNAs 24 and 27 suppress allergic inflammation and target a network of regulators of T helper 2 cell-associated cytokine production. *Immunity.* 44:821–832. https://doi.org/10.1016/j.immuni.2016.01.003

Rao, P.K., Y. Toyama, H.R. Chiang, S. Gupta, M. Bauer, R. Medvid, F. Reinhardt, R. Liao, M. Krieger, R. Jaenisch, et al. 2009. Loss of cardiac microRNA-mediated regulation leads to dilated cardiomyopathy and heart failure. *Circ. Res.* 105:585–594. https://doi.org/10.1161/CIRCRESAHA.109.200451

Regelin, M., J. Blume, J. Pommerencke, R. Vakilzadeh, K. Witzlau, M. Łyszkiewicz, N. Ziętara, N. Saran, A. Schambach, and A. Krueger. 2015. Responsiveness of developing T cells to IL-7 signals is sustained by miR-17:d. *J. Immunol.* 195:4832–4840. https://doi.org/10.4049/jimmunol.1402248

Rusca, N., L. Dehò, S. Montagner, C.E. Zielinski, A. Sica, F. Sallusto, and S. Monticelli. 2012. MiR-146a and NF-κB1 regulate mast cell survival and T lymphocyte differentiation. *Mol. Cell. Biol.* 32:4432–4444. https://doi.org/10.1128/MCB.00824-12

Scanlon, S.T., and A.N.J. McKenzie. 2012. Type 2 innate lymphoid cells: New players in asthma and allergy. *Curr. Opin. Immunol.* 24:707–712. https://doi.org/10.1016/j.coi.2012.08.009

Simpson, L.J., S. Patel, N.R. Bhakta, D.F. Choy, H.D. Brightbill, X. Ren, Y. Wang, H.H. Pua, D. Baumjohann, M.M. Montoya, et al. 2014. A microRNA upregulated in asthma airway T cells promotes TH2 cytokine production. *Nat. Immunol.* 15:1162–1170. https://doi.org/10.1038/ni.3026

Smith, S.G., R. Chen, M. Kjarsgaard, C. Huang, J.-P. Oliveria, P.M. O'Byrne, G.M. Gauvreau, L.P. Boulet, C. Lemiere, J. Martin, et al. 2016. Increased numbers of activated group 2 innate lymphoid cells in the airways of patients with severe asthma and persistent airway eosinophilia. *J. Allergy Clin. Immunol.* 137:75–86.e8. https://doi.org/10.1016/j.jaci.2015.05.037

Steiner, D.F., M.F. Thomas, J.K. Hu, Z. Yang, J.E. Babiarz, C.D.C. Allen, M. Matloubian, R. Blelloch, and K.M. Ansel. 2011. MicroRNA-29 regulates T-box transcription factors and interferon-γ production in helper T cells. *Immunity.* 35:169–181. https://doi.org/10.1016/j.immuni.2011.07.009

Thai, P., Y. Chen, G. Dolganov, and R. Wu. 2005. Differential regulation of MUC5AC/Muc5ac and hCLCA-1/mGob-5 expression in airway epithelium. *Am. J. Respir. Cell Mol. Biol.* 33:523–530. https://doi.org/10.1165/rcmb.2004-0220RC

Van Dyken, S.J., J.C. Nussbaum, J. Lee, A.B. Molofsky, H.-E. Liang, J.L. Pollack, R.E. Gate, G.E. Haliburton, C.J. Ye, A. Marson, et al. 2016. A tissue checkpoint regulates type 2 immunity. *Nat. Immunol.* 17:1381–1387. https://doi.org/10.1038/ni.3582

von Moltke, J., and R.M. Locksley. 2014. I-L-C-2 it: type 2 immunity and group 2 innate lymphoid cells in homeostasis. *Curr. Opin. Immunol.* 31:58–65. https://doi.org/10.1016/j.coi.2014.09.009

Walker, J.A., and A.N.J. McKenzie. 2013. Development and function of group 2 innate lymphoid cells. *Curr. Opin. Immunol.* 25:148–155. https://doi.org/10.1016/j.coi.2013.02.010

Williams, Z., I.Z. Ben-Dov, R. Elias, A. Mihailovic, M. Brown, Z. Rosenwaks, and T. Tuschl. 2013. Comprehensive profiling of circulating microRNA via small RNA sequencing of cDNA libraries reveals biomarker potential and limitations. *Proc. Natl. Acad. Sci. USA.* 110:4255–4260. https://doi.org/10.1073/pnas.1214046110

Wong, S.H., J.A. Walker, H.E. Jolin, L.F. Drynan, E. Hams, A. Camelo, J.L. Barlow, D.R. Neill, V. Panova, U. Koch, et al. 2012. Transcription factor RORα is critical for nuocyte development. *Nat. Immunol.* 13:229–236. https://doi.org/10.1038/ni.2208

Xiao, C., L. Srinivasan, D.P. Calado, H.C. Patterson, B. Zhang, J. Wang, J.M. Henderson, J.L. Kutok, and K. Rajewsky. 2008. Lymphoproliferative disease and autoimmunity in mice with increased miR-17-92 expression in lymphocytes. *Nat. Immunol.* 9:405–414. https://doi.org/10.1038/ni1575

Yang, L., M.P. Boldin, Y. Yu, C.S. Liu, C.-K. Ea, P. Ramakrishnan, K.D. Taganov, J.L. Zhao, and D. Baltimore. 2012. miR-146a controls the resolution of T cell responses in mice. *J. Exp. Med.* 209:1655–1670. https://doi.org/10.1084/jem.20112218